CHARACTERIZATION OF PRECIPITATES ASSOCIATED WITH BITUMONOUS COAL MINE DRAINAGE, NORTHERN APPALACHIAN REGION, USA

by

Candace Lianne Kairies

BS, Westminster College, 1996

MS, Duquesne University, 1998

Submitted to the Graduate Faculty of

Geology and Planetary Science in partial fulfillment

of the requirements for the degree of

Doctor of Philosophy

University of Pittsburgh

2003

UNIVERSITY OF PITTSBURGH

FACULTY OF ARTS AND SCIENCES

This dissertation was presented

by

Candace Lianne Kairies

It was defended on

June 7, 2002

and approved by

Dr. Robert S. Hedin

Dr. Edward G. Lidiak

Dr. Harold B. Rollins

Dr. Brian W. Stewart

Dr. Rosemary C. Capo
Dissertation Director

CHARACTERIZATION OF PRECIPITATES ASSOCIATED WITH BITUMONOUS COAL MINE DRAINAGE, NORTHERN APPALACHIAN REGION, USA

Candace L. Kairies, Ph.D.

University of Pittsburgh, 2003

Changes in precipitate mineralogy, morphology, and major and trace elemental concentrations and associations throughout five coal mine drainage remediation systems in Pennsylvania and Maryland that treat discharges of varying chemistries were investigated. The precipitates are dominantly (>70%) goethite with minor amounts of other iron and/or manganese oxides and quartz. Crystallinity varies throughout an individual system and is a function of the treatment system and how rapidly ferrous iron oxidizes, precipitates, and settles. Precipitates formed earlier in the systems have the highest crystallinity; less crystalline precipitates are associated with enhanced sorption of trace metals. High surface area and vacancies within the goethite structure enable incorporation of metals from mine drainage polluted waters. Sorption affinities follow the order Al>Zn>Co≈Ni>Mn. As pH increases in the individual treatment systems toward the pH_{pzc}, arsenic sorption decreases and aluminum and transition metal sorption increases. Sulfate, sodium and ferrous iron potentially influence the sorption of trace metals.

A sequential extraction procedure was developed to determine how trace elements are associated with the precipitates. Arsenic, cobalt, manganese, nickel and zinc are not released until the iron hydroxide phase is dissolved, indicating these metals are either tightly sorbed to the surface or incorporated into the hydroxide structure. Cobalt and nickel preferentially partition into a manganese oxide/hydroxide phase (if present), over the iron hydroxide phase. The stability of

the precipitate controls the long-term mobility of trace metals. Associated trace metals will remain unavailable to the environment as long as the precipitate is not altered.

Additionally, spatial and temporal variations between precipitates formed from a net-alkaline coal mine discharge were examined. The precipitates are all moderately crystalline goethite with minor variations in morphology and composition. They contain 20 – 30% more iron than the natural mined iron oxides examined in this study, and concentrations of manganese, nickel and zinc are up to three orders of magnitude lower than the natural iron oxides. Geochemical analysis indicates that mine drainage precipitates formed from net-alkaline waters are of a higher purity than natural iron oxides. Results of this study have implications for disposal, resource recovery, and the optimization of mine drainage passive remediation systems.

ACKNOWLEDGEMENTS

I owe a special thank you to Dr. Kenneth Long for introducing me to the field of geology and helping me to discover what path in life to take, even though it took a few years to find it.

I am forever indebted to my advisor, Dr. Rosemary C. Capo, for her guidance and support. Without her I would not be the person I am today. I also want to thank the other members of my committee, particularly Dr. Brian Stewart whose efforts greatly improved this work, as well as Dr. Robert Hedin, Dr. Harold Rollins and Dr. Edward Lidiak for their helpful comments and suggestions.

Much appreciation is extended to George Watzlaf of the U.S. Dept. of Energy/National Energy Technology Laboratory for being my mentor in the University Partnership Program and for teaching me most everything I know about mine drainage treatment.

Brian K. Games provided assistance in the laboratory above and beyond the call of duty. Without his technical expertise, I would still be in the lab.

I also want to acknowledge the help and support provided by Gregory Radencic, Laura Homsey, Paula Grgich, Ann Kim and Karl Schroeder.

Finally, I extend a special thank you to three important people in my life: Sherry Stafford for showing me the ropes when I first began my graduate career, assistance in sampling (even though you chose to take pictures of me in the muck instead of pulling me out!) and friendship; Jennifer Piatek for tech support at odd hours of the morning and being a great friend; and Lee Beatty not only for assistance in sampling (especially saving me from drowning), but also for friendship, support and other things too numerous to mention here.

This work is dedicated to my mom and the friends who gave me the love and support I needed along the way. I also dedicate this work in memory of Michael Santabarbara who never had the chance to realize his dreams.

TABLE OF CONTENTS

LIST OF TABLES

LIST OF FIGURES

Chapter 1

Characterization of Precipitates Formed in Passive Treatment Systems

I. Introduction

Drainage from abandoned mined lands (AML) remains a widespread problem in the Appalachian coal fields, with about 3900 km of streams affected by coal mine drainage (CMD) in Pennsylvania alone (PA Department of Environmental Protection, 1998). Coal mine drainage can contain acidity, sulfates and metals, including iron (Fe), aluminum (Al) and manganese (Mn), as well as arsenic (As), cobalt (Co), nickel (Ni), and zinc (Zn). It is estimated that over 100,000 tons of iron are discharged from coal mines each year in the United States (Hedin, 1996).

The oxidation of pyrite exposed during mining and the subsequent oxidation and hydrolysis of iron produces hydroxide precipitates such as goethite (α-FeOOH), lepidocrocite (γ-FeOOH), schwertmannite ($Fe_{16}O_{16}(OH)_y(SO_4)_z \cdot nH_2O$) and ferrihydrite ($Fe_5HO_8 \cdot 4H_2O$), depending on pH conditions. These precipitates can coat the bottoms of streams and smother aquatic life. Schwertmannite is the main mineral formed in acidic mine drainage with pH between 3.0 and 4.5, while ferrihydrite and goethite form at pH>5.0 and 6.0, respectively (Bigham et al., 1992). Both schwertmannite and ferrihydrite are metastable with respect to goethite and will eventually transform to goethite over time (Bigham et al., 1992).

Iron hydroxides generally exist as colloidal particles with high surface to volume ratios; thus they have a high specific surface area (Cornell and Schwertmann, 1996). As a result, they tend to be excellent sorbents of trace metals (e.g., As, Co, Ni, and Zn) and subsequently can control

their mobility, fate and transport in polluted and unpolluted waters (Carlson and Schwertmann, 1981; Chapman et al., 1983; Blowes and Jambor, 1990; Herbert, 1996).

Various treatment methods have been developed to remediate CMD contaminated water. Active treatment involves the addition of alkaline chemicals (e.g., sodium hydroxide or ammonia), to raise pH and precipitate metals. Passive treatment methods utilize chemical and biological processes that occur naturally to clean the water. Such methods usually consist of multiple unit operations selected based on the chemistry of the discharge. Waters that are net alkaline (alkalinity > acidity) can be passively treated using a series of ditches, ponds and aerobic wetlands to aerate and detain water and allow iron to oxidize, precipitate and settle (Watzlaf et al., 2000). Net acidic waters must first be neutralized, which can be achieved through the dissolution of limestone and/or microbial processes. A variety of techniques have been developed to promote alkalinity generation, including the use of either an anoxic limestone drain (ALD) or a vertical flow wetland (VFW), also referred to as Reducing and Alkalinity-Producing Systems (RAPS), or Successive Alkalinity-Producing Systems (SAPS).

ALDs are buried beds of limestone designed to add alkalinity to anoxic waters that contain <1 mg/L of dissolved Al and ferric iron (Fe^{3+}) through limestone dissolution (Turner and McCoy, 1990). Dissolved Al (if present) precipitates at pH values between 4.5 and 8.5 (Stumm and Morgan, 1970), and subsequently clogs the ALD. If dissolved oxygen is present, then dissolved ferrous iron (Fe^{2+}) can oxidize and precipitate, which also clogs the ALD. ALDs are usually followed by ponds and aerobic wetlands to allow the iron to oxidize, precipitate and settle.

VFW/RAPS/SAPS consist of limestone overlain by compost and water. Drain pipes within the limestone layer cause the downward flow of water through the compost and the limestone. Microbial reduction of sulfate in the organic compost layer and limestone dissolution generate

alkalinity. Because of the reducing conditions in the compost layer, these systems are appropriate for waters that contain ferric iron, as it is reduced to the ferrous form, preventing the precipitation of ferric hydroxides.

Over time, the ponds and wetlands used in CMD treatment systems accumulate iron-rich solids, and their ability to treat contaminated water is reduced. Most passive systems are constructed to hold 10 – 30 years of precipitates. The pond sludge must eventually be cleaned out in order to maintain treatment effectiveness, resulting in removal and disposal costs. These costs can be offset if the iron hydroxides could be recovered and used as a resource. However, the precipitates must be fully characterized in order to determine an appropriate end use or disposal method.

Properties of iron hydroxides have been examined in detail, including their formation and occurrence in natural and metal contaminated waters (Herbert, 1996; Childs et al., 1998; Hudson-Edwards et al., 1999) and their mineralogy and morphology (Schwertmann et al., 1985; Gerth, 1990; Bigham et al., 1992). Iron oxide content of precipitates in mine drainage treatment wetlands has also been examined in relation to color (Tarutis and Unz, 1994) and mineralogy/morphology (Karathanasis and Thompson, 1995). Numerous investigations into the sorptive properties of synthetic iron oxides have also been conducted (Benjamin and Leckie, 1980; Balistrieri and Murray, 1982; Ali and Dzombak, 1996a; Webster et al., 1998). The physical parameters (settleability, particle size, viscosity, specific resistance and wet packing density) of mine drainage precipitates have also been examined (Jeon, 1998). However, no study has characterized and compared the chemical and physical properties of the precipitates that form within CMD passive treatment systems. Here changes in precipitate mineralogy, morphology, and major and trace elemental concentrations and associations throughout five

systems treating discharges of varying chemistries are investigated. The goal is to create a predictive model for the type of precipitates formed in passive systems with implications for improvement in design of passive systems as well as resource recovery.

2. Treatment Systems

The five passive treatment systems (Morrison II, Howe Bridge, Elklick, P-A, Scrubgrass) sampled in this study are located in the Bituminous coal fields of western Pennsylvania and northern Maryland (Figure 1), and treat discharges from Pennsylvanian age coals (Figure 2). Morrison II (Figure 3a; Clarion coal) treats drainage off a reclaimed surface mine. Water is captured and sent through an anoxic limestone drain (ALD) before traveling through a serpentine ditch. At Howe Bridge (Figure 3b; Clarion coal), discharge from an abandoned gas well is piped to an ALD, and then sent through two ponds, a wetland and a reducing and alkalinity-producing system (RAPS). At Elklick (Figure 3c; Kittanning coal), water from an abandoned borehole is collected and sent through an ALD followed by a pond, ditch and wetland. Water at the P-A site (Figure 3d; Freeport coal) is aerated by a blower and then flows into a pond, down a ditch and into two additional ponds. At the Scrubgrass site (Figure 3e, Pittsburgh coal), water is aerated with a low-pressure system prior to flowing through a pond and wetland. Both the Scrubgrass and P-A systems treat underground mine discharges.

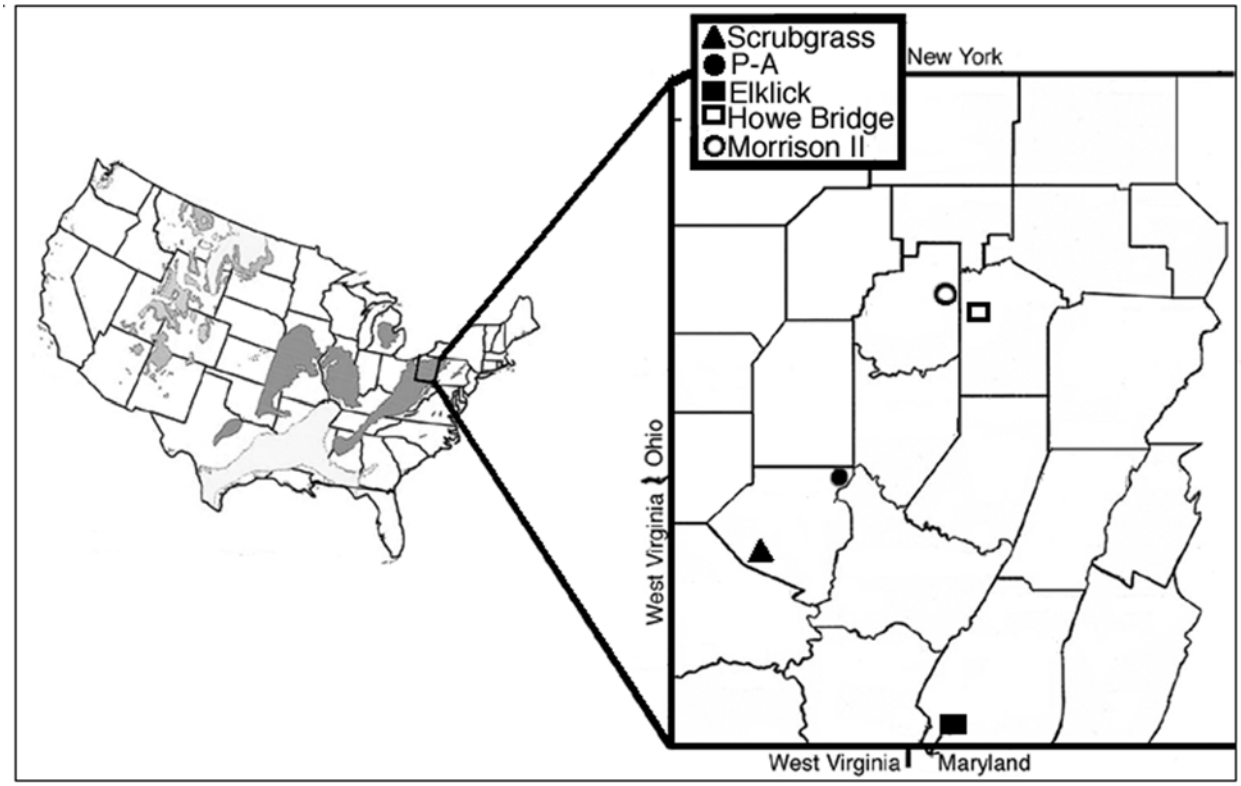

Figure 1. Location of passive treatment systems sampled in this study.

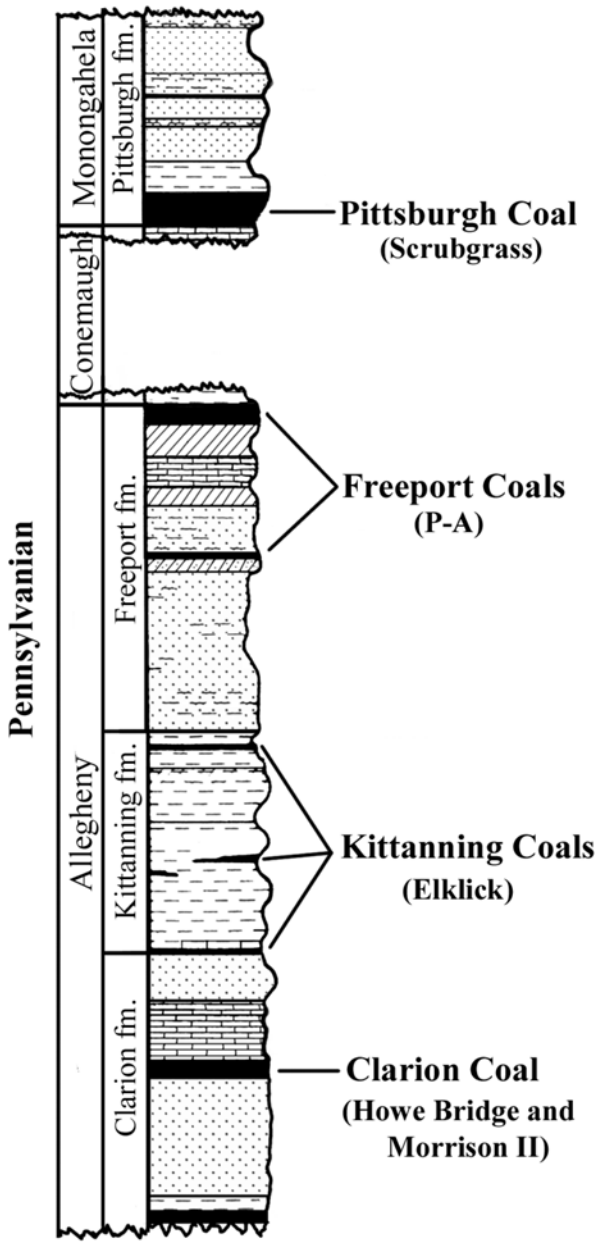

Figure 2. General stratigraphy of Pennsylvanian coals.

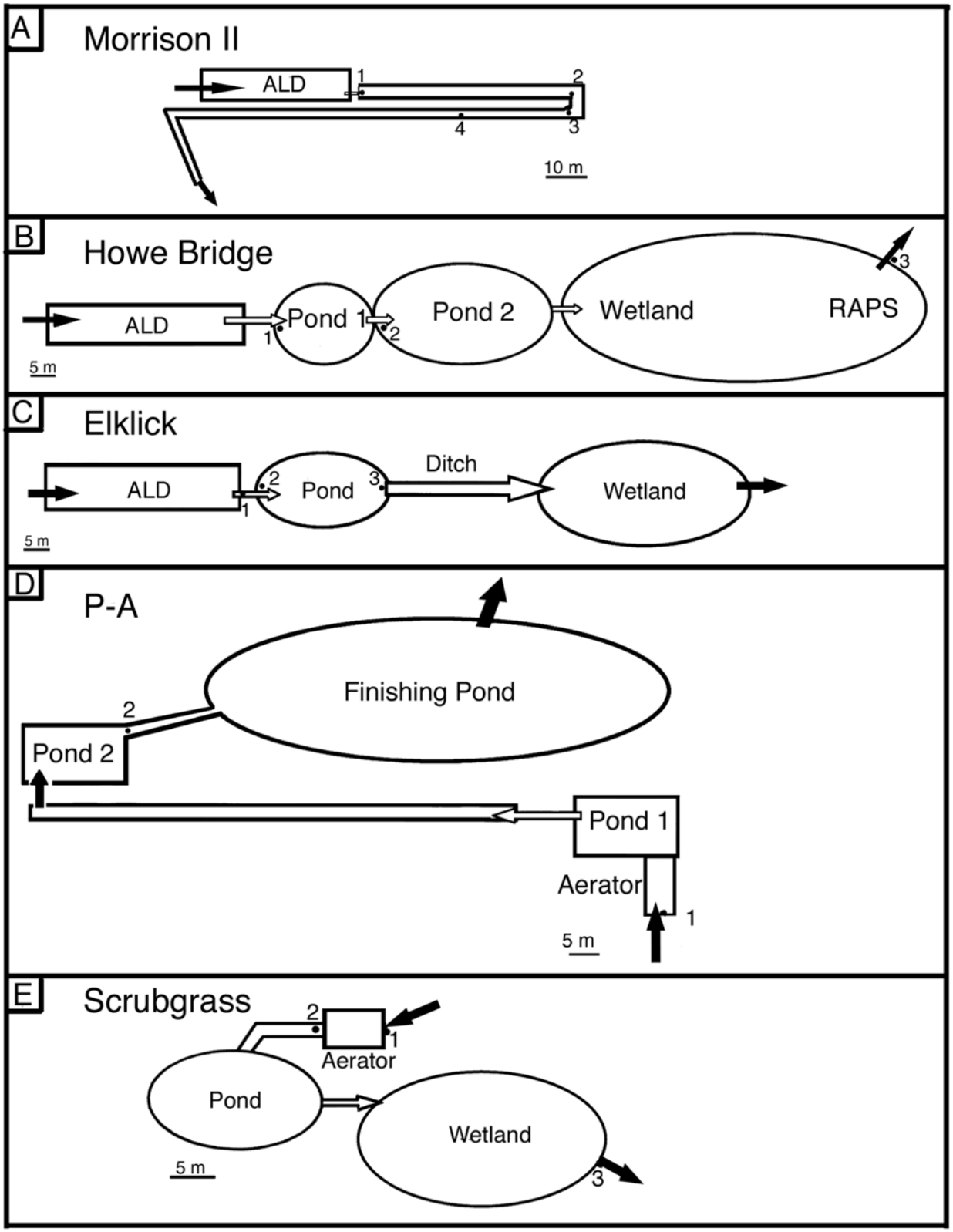

Figure 3. Schematics of passive treatment systems and sampling points; arrows indicate flow direction: (a) Morrison II; (b) Howe Bridge; (c) Elklick; (d) P-A; (e) Scrubgrass.

3. Methodology

3.1. Sampling and sample preparation

Water samples were collected for metals analysis at each sampling location. Samples were filtered through a 0.2-micron syringe cellulose acetate filter and acidified in the field to pH<2 with HCl. Field pH was measured using an Orion 250A pH meter; field alkalinity was determined using either the Orion® Total Alkalinity Test Kit with a calibrated pH meter, or the Hach® digital titration method.

Grab samples of the precipitates (representing up to several years of accumulation) were collected in 1L HDPE bottles, bags or glass sampling containers. In the laboratory, visible organic matter was removed by hand and splits of the precipitate samples were dried at <40˚C to prevent volatilization and potential loss of structural water.

3.2. Chemical and physical analysis

Trace and major element concentrations in the water samples were determined using inductively coupled plasma-atomic emission spectroscopy (ICP-AES) at the University of Pittsburgh Geochemistry Laboratory and at the U.S. Department of Energy/National Energy Technology Laboratory (U. S. DOE/NETL), using a SpectroFlame and Perkin-Elmer Optima 3000, respectively. Sulfate concentrations were determined by ion chromatography or from total sulfur measured by ICP-AES. Ferrous iron concentrations were determined by titration with $K_2Cr_2O_7$ (method of Fales and Kenny, 1940).

Total metals in the precipitate samples were determined through instrumental neutron activation analysis (INAA) and total acid digestion followed by analysis using ICP-AES at

Activation Laboratories in Ontario, Canada. X-ray diffraction (XRD) patterns were obtained at the University of Pittsburgh Materials Science Laboratory using a Phillips X'pert powder diffractometer with Cu Kα radiation. Back-filled powder mounted samples were scanned from 5 to 15˚ 2θ using a 0.5˚ divergence slit and from 15 - 75˚ 2θ using a 1.0˚ divergence slit. Peak positions (d-spacings) were determined using the Phillips X'pert Organizer software. Morphology was determined using a Phillips XL30 FEG scanning electron microscope (SEM) with EDAX, also at the Materials Science Laboratory.

4. Results

4.1. Water chemistry

Water quality data (Table 1) collected from Howe Bridge and Elklick were averaged with long-term water quality data from the U. S. DOE NETL in order to obtain representative average water chemistry at these sites. Averages were used because the precipitate samples from these systems potentially represent years of deposition. Depending on the removal rate of iron (wetlands are usually sized to remove 10 – 20 g/d/m^2; Hedin et al., 1994), an average of 3 - 5 cm of precipitate accumulates annually in ponds and wetlands. Waters collected from Scrubgrass, P-A and Morrison II are from one sampling event, as these sites were recently constructed and put into operation at the time of sampling, so no long-term data are available. However, data from the other sites suggest there have been no major variations in water chemistry over the 5 – 10 year period the systems have been in operation.

Raw (influent) water quality data are indicated in the table and are included even though precipitates may not have been formed at this point. Influent water cannot be sampled at the

Morrison II site as the water is piped directly into an anoxic limestone drain with no external access. As can be seen in Table 1, the raw (influent) water quality in these systems varies considerably between sites, with Fe ranging from 56 – 270 mg/L; Mn from 0.7 – 41 mg/L; Al from <0.10 - 1.4 mg/L and concentrations of Co, Ni and Zn ranging from <0.005 up to 1.5 mg/L.

Table 1. Passive treatment system water chemistry (mg/L).

System and Sample Location	pH su	Alkalinity (mg/L $CaCO_3$)	Fe^{2+}	Tot Fe	Al	Ca	Co	K	Mg	Mn	Na	Ni	Zn	SO_4^{2-}
Clarion Coal														
Morrison II														
1	5.89	149	215.4	215.4	0.5	200.6	0.71	6.2	117.0	40.7	5.2	0.84	1.49	1200
2	5.97	nd	217.9	217.9	0.5	193.8	0.71	6.2	116.2	40.8	4.9	0.84	1.51	1204
3	6.34	nd	209.2	255.6	1.4	195.2	0.74	6.2	116.0	40.9	5.0	0.86	1.64	1214
4	6.37	nd	190.2	194.7	0.3	196.3	0.73	6.4	116.5	41.1	5.2	0.93	1.45	1217
Howe Bridge														
Raw	5.72	33	270.2	269.7	0.1	154.2	0.44	6.1	106.2	41.1	10.5	0.49	0.58	1294
1	6.37	121	246.5	245.8	0.1	200.0	0.44	6.1	102.5	39.7	10.0	0.51	0.57	1261
2	6.38	115	237.9	238.0	0.1	201.6	0.39	5.9	101.9	38.9	12.5	0.43	0.43	1238
3	5.94	62	69.9	71.1	0.3	234.7	0.13	6.1	95.9	34.7	11.9	0.12	0.17	1083
Kittanning Coal														
Elklick														
Raw	6.01	35	54.7	56.0	<0.10	79.3	0.07	2.1	22.1	4.7	1.8	0.10	0.14	336
1	6.64	156	51.0	54.6	<0.10	129.4	0.07	2.1	22.2	4.8	1.6	0.08	0.08	332
2	6.74	nd	41.1	42.4	<0.10	126.0	0.07	2.1	22.5	4.6	1.7	0.08	0.09	344
3	6.93	83	6.5	8.5	<0.10	129.0	0.05	2.1	22.2	4.4	1.8	0.07	0.05	333
Freeport Coal														
P-A														
1 (Raw)	6.79	444	nd	80.6	<0.10	178.9	0.028	8.71	38.7	1.6	781.6	0.04	0.135	1849
2	7.42	nd	nd	11.3	<0.10	179.4	0.027	8.88	39.5	1.6	789.5	0.04	0.015	1881
Pittsburgh Coal														
Scrubgrass														
1 (Raw)	6.11	190	nd	66.3	<0.10	94.5	<0.015	5.4	32.9	0.6	296.0	<0.015	0.17	544
2	6.63	184	nd	42.4	<0.10	96.8	<0.015	5.5	33.2	0.6	293.0	<0.015	0.03	544
3	6.66	190	nd	32.8	<0.10	98.6	<0.015	5.6	33.6	0.6	295.0	<0.015	0.02	543

As<DL of 0.2 mg/L for all samples
nd=not determined

4.2. Mineralogy and morphology

Mineralogy of the precipitates is presented in Table 2. For all samples, the main mineral present is goethite, although Howe Bridge (HB-2 and HB-3) and Morrison II (MOR-2 and MOR-3) samples contain minor amounts of lepidocrocite. Quartz, present in many of the precipitates, represents siliciclastic input (from weathering processes) into the treatment system. The ponds and wetlands are open to input from the surrounding area and exogenous material may be washed in during storm events, though such input is likely minimal. Precipitate crystallinity decreases (XRD peaks become broader and less intense) from the beginning to the end of the treatment systems (e.g., Elklick, Figure 4), with the exception of the Morrison II system, in which crystallinity increases.

Three general morphological categories are present: spherical (either spiky or globular), acicular, and platy; the first two of which occur as aggregates ranging in size from 0.5 to 2 microns. Representative SEM micrographs are shown in Figures 5 - 8. The spiky (Figure 5), globular (Figure 6), and acicular particles (Figure 7) are characteristic of goethite (Domingo et al., 1994; Cornell and Schwertmann, 1996; Webster et al., 1998). Platy particles (Figure 8) are likely lepidocrocite (Domingo et al., 1994; Cornell and Schwertmann, 1996). Other particles include jagged quartz crystals up to 100 microns in diameter (identified by SEM-EDAX and confirmed by XRD). The size and morphology is consistent with detrital quartz rather than authigenic silica (e.g., Roscoe, 1999).

Table 2. Precipitate mineralogy.

		Mineralogy	
System	Location	major	minor
Morrison	1	goethite	quartz
	2	goethite	lepidocrocite
	3	goethite	lepidocrocite
	4	goethite, quartz	
Howe Bridge	1	goethite	quartz
	2	goethite	quartz, lepidocrocite
	3	goethite	quartz, lepidocrocite
Elklick	1	goethite	quartz
	2	goethite	
	3	goethite	
P-A	1	goethite	
	2	goethite, quartz	
Scrubgrass	1	goethite	quartz
	2	goethite	
	3	goethite	

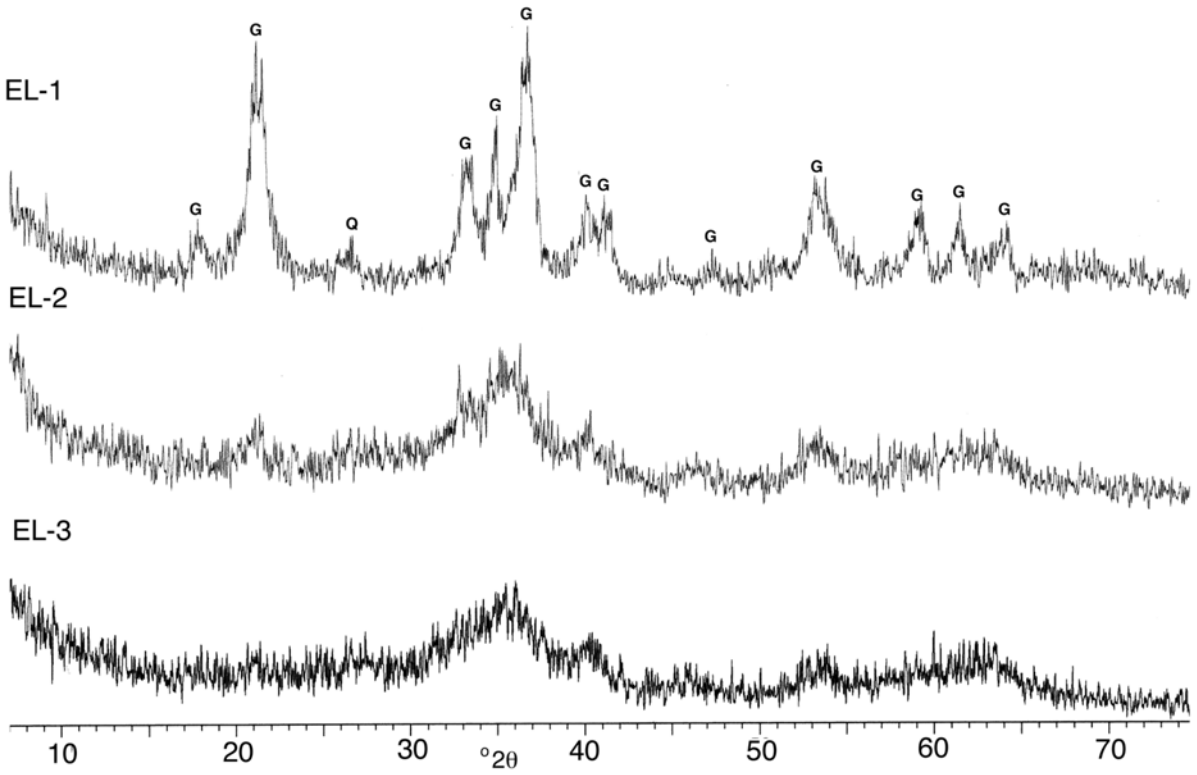

Figure 4. Diffraction patterns of samples collected at Elklick. Crystallinity decreases from EL-1 (closer to influent) to EL-3 (furthest from influent). G = goethite, Q = quartz

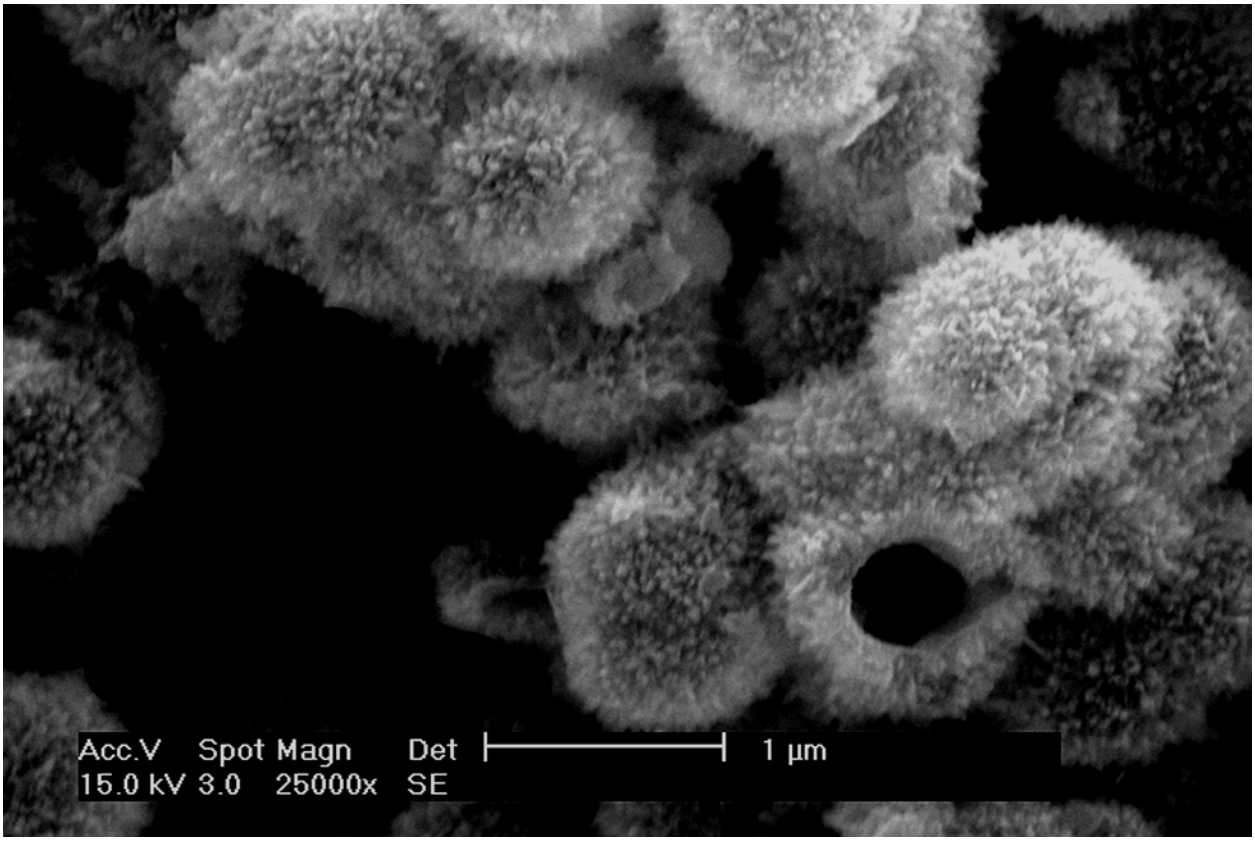

Figure 5. Spiky morphology seen in precipitates collected from passive treatment systems.

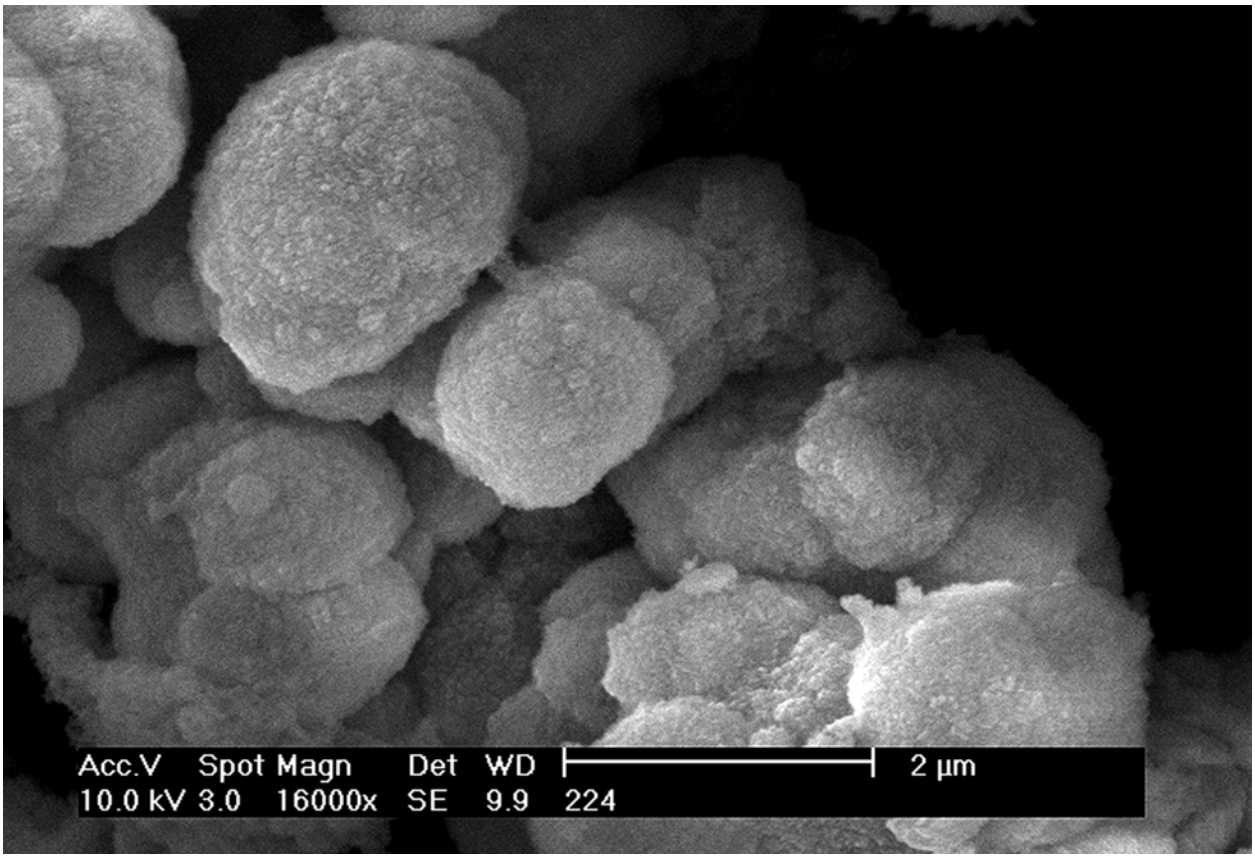

Figure 6. Globular morphology seen in precipitates collected from passive treatment systems.

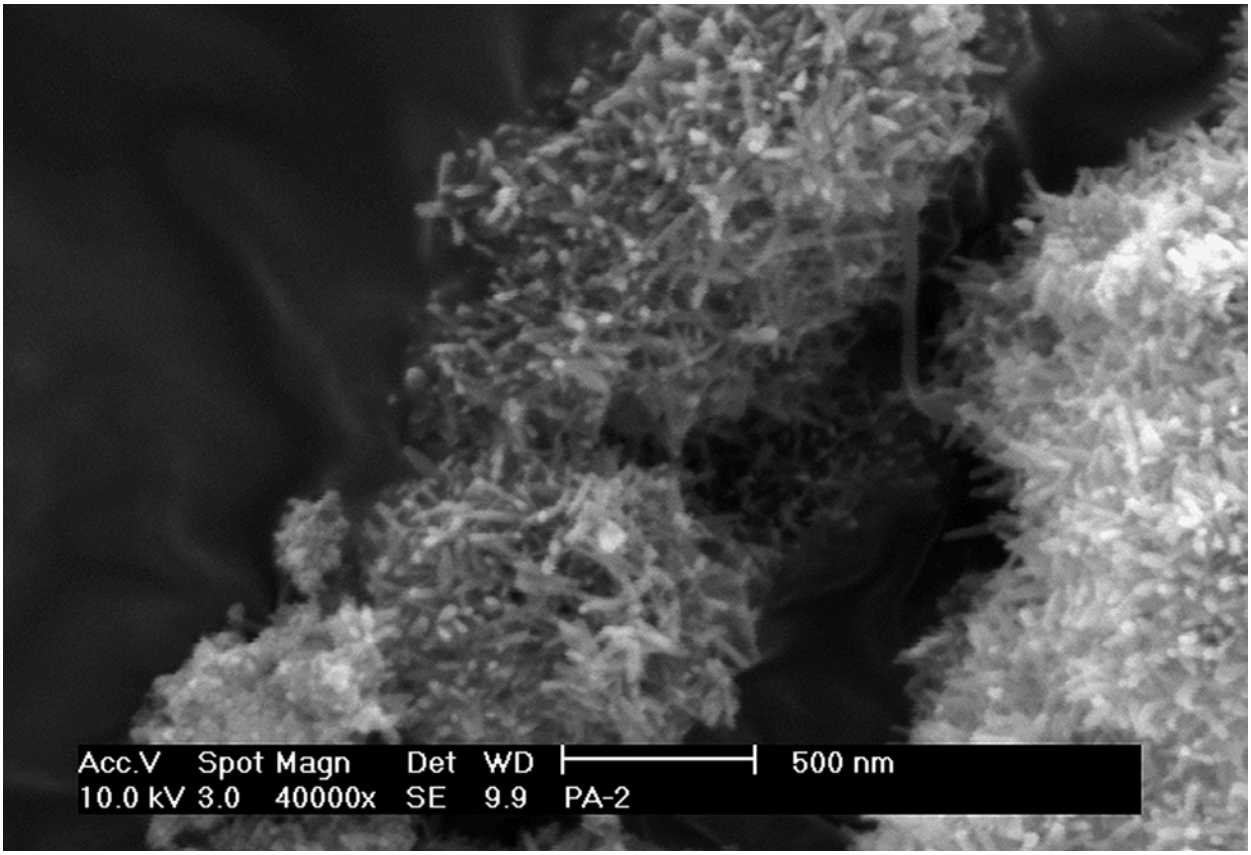

Figure 7. Acicular morphology seen in precipitates collected from passive treatment systems.

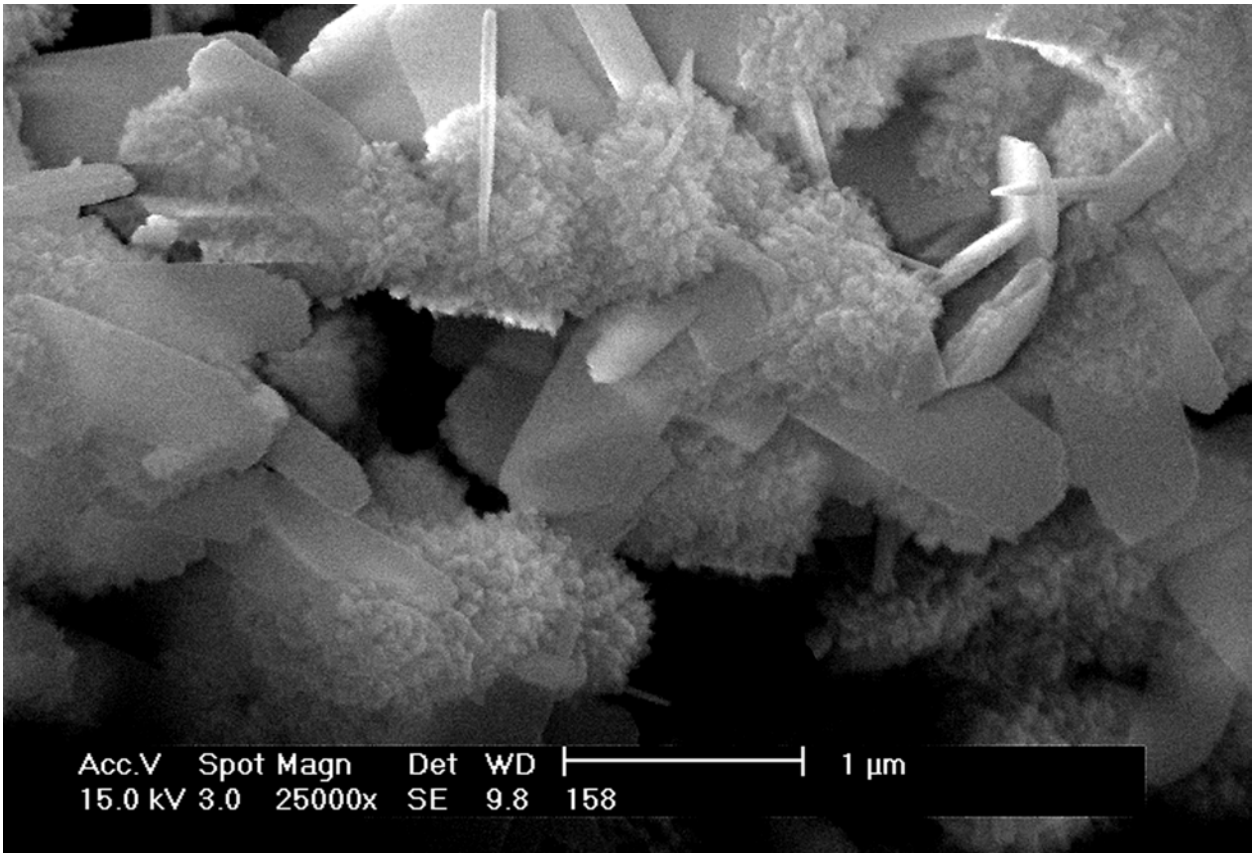

Figure 8. Platy and spiky morphologies seen in precipitates collected from passive treatment systems.

4.3. Precipitate chemistry

4.3.1. Trends within an individual treatment system

Trace and major elemental composition of the bulk precipitates are presented in Table 3. Iron content ranges from 42 - 57%, with varying amounts of aluminum (up to 1.05 wt.%), arsenic (up to 3010 mg/kg), cobalt (up to 936 mg/kg), manganese (up to 3.6 wt.%), nickel (698 mg/kg) and zinc (up to 2400 mg/kg). It is known that naturally occurring goethite rarely exists as pure α-FeOOH, as it usually contains cations such as Al, Co, Ni, and Zn that have been incorporated into the structure (Kühnel et al., 1975; Burns and Burns, 1977).

In all five systems sampled for this study, arsenic (present as either arsenate or arsenite anions in the discharges) in the precipitates decreases from the influent to the effluent of each system. The precipitates are enriched in Al, As, Co, Mn, Ni, Zn and other elements relative to their associated waters (Tables 1, 3). Cobalt, manganese, nickel and zinc concentrations in the precipitates increase as the water flows through the treatment systems with the exception of Morrison II, where the concentrations of these metals decrease.

4.3.2. Comparison between passive treatment systems

Variations in the trace metal content of precipitates are also seen between treatment systems, with certain systems exhibiting greater concentrations than other systems. Precipitates from Elklick contain the highest concentrations of Mn, Co, and Ni, while those from Morrison II contain the highest amounts of Al and Zn. Arsenic concentration is greatest in the Scrubgrass and P-A precipitates.

Table 3. Precipitate chemistry in wt.% (where noted) or mg/kg.

System and Sample Location		FeOOH%	Fe%	Al%	Ca%	K %	Mg%	Na%	P%	S %	As	Co	Mn	Ni	Pb	Zn
Clarion Coal																
Morrison II																
	1	77	49	1.05	0.21	0.03	<0.01	0.01	0.003	0.77	119	92	1216	189	40	2400
	2	87	55	0.51	0.06	0.04	<0.01	<0.01	<0.001	0.71	34	69	1080	90	31	2240
	3	86	54	0.44	0.06	0.05	<0.01	0.01	<0.001	1.29	28	40	645	42	34	1500
	4	74	47	1.05	0.07	0.26	<0.01	0.03	0.003	1.59	34	26	440	28	34	1000
Howe Bridge																
	1	87	55	0.04	<0.01	<0.01	<0.01	0.03	0.039	0.99	11	34	1550	37	21	303
	2	91	57	0.04	<0.01	<0.01	<0.01	0.03	0.036	1.13	19	25	1294	29	29	405
	3	80	50	0.19	0.20	<0.01	0.02	0.03	0.802	0.59	0	27	2265	50	27	177
Kittanning Coal																
Elklick																
	1	85	54	<0.01	0.18	<0.01	<0.01	0.02	0.067	0.35	11	68	1645	70	23	202
	2	81	51	0.01	0.19	0.01	<0.01	0.02	0.051	0.34	15	126	4030	128	13	554
	3	67	42	0.12	0.64	0.07	0.02	0.03	0.024	0.21	6	936	35928	698	32	757
Freeport Coal																
P-A																
	1	90	56	0.01	0.64	<0.01	<0.01	0.56	0.022	0.632	327	22	387	37	41	70
	2	79	50	0.47	2.14	0.13	0.06	0.47	0.006	0.445	114	56	1040	80	38	140
Pittsburgh Coal																
Scrubgrass																
	1	80	50	0.37	0.24	0.10	0.04	0.20	0.212	0.43	3010	4	80	10	21	38
	2	78	49	0.56	<0.01	0.18	0.02	0.09	0.027	0.29	437	4	84	11	31	39
	3	85	53	0.10	<0.01	0.04	<0.01	0.06	0.010	0.25	121	6	312	6	20	94

5. Discussion

5.1. Partitioning of Trace Elements

Distribution coefficients (K_d) are used to quantify equilibrium metal partitioning. However, such calculations are useful only for the specific conditions under which they are measured and cannot be applied to other systems (Honeyman and Leckie, 1986; Rose and Bianchi-Mosquera, 1993). Additionally, in the passive treatment systems it cannot be assumed there is equilibrium between the water and the precipitate, and that transport has not occurred. Munk et al. (2002) studied trace element distribution in Al hydroxides precipitated from polluted mine waters. They used a concentration ratio (CR) to explain trace element distribution:

$$CR = [X]_s/[X]_l$$

where X represents the concentration of a particular element in the solid ($[X]_s$) and aqueous ($[X]_l$) phase. While the formulation is the same as K_d, the use of the term CR does not assume equilibrium between waters and coexisting solids.

In this study, concentration ratios allow for comparison of precipitate enrichment as well as the distribution of elements between the solid and liquid phase (where trends may not be obvious by looking at precipitate and water chemistry alone) not only within a treatment system, but also between systems. If an element was below the detection limit (DL) in the water, the DL was assumed to be the maximum concentration of this element. Concentration ratios were not determined for elements below DL in the precipitate.

Precipitates from Howe Bridge (Figure 9a), Elklick (Figure 9b), Scrubgrass (Figure 9c) and P-A (Figure 9d) generally become increasingly enriched through the treatment system in Al, Co, Mn, Ni and Zn relative to the associated mine waters. The exception is the Morrison II system (Figure 9e), where enrichment in the precipitates generally decreases relative to the water

through the treatment system. Arsenic in the precipitates decreases in the P-A (Figure 9d) and Scrubgrass systems (Figure 9c).

In this study, metal affinities for the goethite surface (determined by log CR) generally follow the order:

$$Al > Zn > Co \approx Ni > Mn$$

Although the CR values vary between systems, the order of sorption affinity remains the same. These results are comparable to experimental and modeled K_d values (Cr > Pb > Cu > Zn > Ni > Ca) determined by Dzombak and Morel (1990) and work on synthetic goethite (Cu > Pb > Zn > Co > Ni > Mn > Ca >Mg) by Gerth (1990) and Cornell and Schwertmann (1996).

Given that the log CR values of the CMD precipitates are comparable to log K_d laboratory values, and that iron hydroxides are excellent sorbents of ions (Balistrieri and Murray, 1982), it is likely that the trace metal associations seen in the passive treatment precipitates are related to sorption of the metals to the surface of the precipitate. Sorption and the influence of the iron hydroxide surface and structure, the point of zero charge, crystallinity, and other species present in both the water and the precipitates, are examined below.

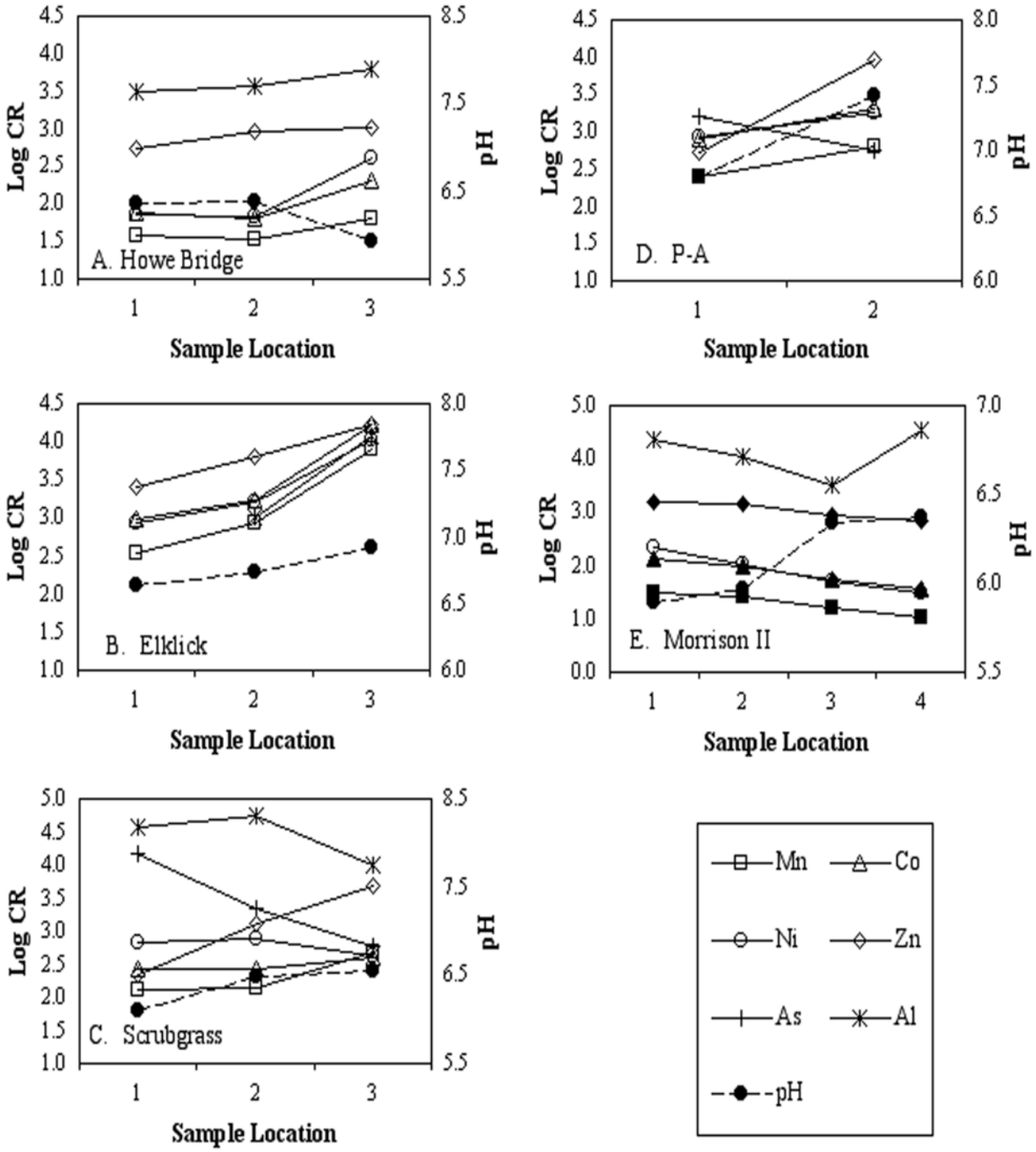

Figure 9. Concentration ratios. (a) Howe Bridge; (b) Elklick; (c) Scrubgrass; (d) P-A; (e) Morrison II. Flow through each system is from left to right on the graph.

5.2. Iron hydroxide surfaces and structures and the point of zero charge

Sorption on iron hydroxide particles is controlled by the surface hydroxyl groups that are singly, doubly or triply coordinated with Fe atoms (Cornell and Schwertmann, 1996). The surface can be positively, negatively or neutrally charged ($FeOH_2^+$, FeO^-, $FeOH^0$) through the adsorption or desorption of protons (pH dependent), making the iron hydroxides amphoteric (Cornell and Schwertmann, 1996). Specific sites are available for anion and cation sorption, and these sites may be physically and electrically isolated from each other (Coughlin and Stone, 1995). Empty surface sites in the goethite structure are often occupied by additional hydroxyl groups, which are also available for reaction (Cornell and Schwertmann, 1996).

Due to the high surface area of the iron hydroxides, numerous sites are available for sorption reactions; the number and type of surface hydroxyl groups available are a function of pH. Sorption of most metals to the iron hydroxide surface is generally followed by diffusion of the metal into internal bonding sites and subsequent incorporation into the iron hydroxide crystal structure, potentially freeing up surface sites for continued sorption (Coughlin and Stone, 1995; Cornell and Schwertmann, 1996).

The pH of the point of zero charge (pH_{pzc}) is the pH at which the net surface charge is equal to zero. A net positive charge exists at $pH < pH_{pzc}$; this results in increased anion sorption. Correspondingly, the net negative charge at $pH > pH_{pzc}$ results in increased cation sorption (Dzombak and Morel, 1990; Cornell and Schwertmann, 1996). Although the pH_{pzc} of natural goethite is unknown, synthetic goethite has been found to have a pH_{pzc} between 7.5 and 9.0 (Yates and Healy, 1975; Zeltner and Anderson, 1988; Jeon, 1998). The pH_{pzc} of natural goethite

is likely similar, but would be affected by the presence of other dissolved species in mine drainage polluted waters.

As water flows through treatment systems, the pH generally increases. For example, at Elklick pH increases from 6.6 to 6.9 (Figure 9b and Table 1), and at Scrubgrass the pH increases from 6.1 to 6.6 (Figure 9c and Table 1). Changes in pH result from alkalinity addition, CO_2 sparging (due to agitation/oxidation of the water) as well as precipitate formation. As the pH_{pzc} of goethite (7.5 – 9.0) is approached, it is expected that positive sorption sites will decrease (resulting in a subsequent decrease in anion sorption), while negative sorption sites will increase (resulting in increased cation sorption). This could account for the decrease in As and increase in metal cations observed in systems in this study. An exception to this is the Howe Bridge site, where pH actually decreases while metal CR values increase (Figure 9a). At Howe Bridge, CR values are lower than at the other sites, which could be due to the decrease in pH. At the Morrison II site (Figure 9e), metal CR trends also do not follow the expected trend with pH. This could be due to changes in crystallinity, as discussed below.

5.3. Sorption and crystallinity

As noted previously, precipitates from the Morrison II system differ from the other treatment systems in that crystallinity increases, and although pH increases from 5.9 to 6.4, concentration ratios of Co, Mn, Ni and Zn decrease from the influent to the effluent (Figure 9e and Table 1). In this system, the increased crystallinity potentially overwhelms the enhanced sorption of trace metal cations associated with rising pH. Low crystallinity and high surface area of minerals such as ferrihydrite make them highly effective at sorbing trace elements from solution (Xu et al., 1997). As the crystals become larger, surface area decreases, which corresponds to fewer

surface sorption sites and a lower sorption capacity. It has been found that the crystal structure of goethite may prohibit metal sorption and release due to its small interatomic spacing (Coughlin and Stone, 1995). At the other sites, the decrease in crystallinity throughout the individual systems corresponds to an increase in trace metal sorption, supporting the idea that the degree of crystallinity affects the degree of sorption. Additionally, increased sorption of trace metals may influence the extent of crystallinity. Increasing oxidation rates can also increase crystallinity. At the Morrison II site, sample locations 2, 3, and 4 are areas of enhanced aeration and increased oxidation, as there is a drop in elevation going around a bend to the lower portion of the ditch. As a result, crystallinity is higher and cation sorption decreases. Although the CR of Al decreases from sampling points 1 – 3 (following the trend of other trace metal cations, there is a sharp increase in enrichment at sampling point 4, which may be related to the high affinity of Al for the goethite surface. Goethite can undergo isomorphic substitution (solid solution) for Fe^{3+} by other trivalent cations, and Al is one of the best known and studied examples of isomorphous substituting constituents (Cornell and Schwertmann, 1996). Aluminum's strong affinity for the goethite surface may lead to the formation of an Al substituted goethite (Cornell and Schwertmann, 1996). Sorption of anions (arsenic) does not appear to be influenced by precipitate crystallinity. In every system, arsenic concentration in the precipitates decreases from the beginning to the end, regardless of crystallinity.

Transformation from one structure to another (e.g. ferrihydrite to goethite, poorly crystalline goethite to crystalline goethite) could result in the release of sorbed and structurally incorporated metals. Aged iron oxyhydroxides do not release sorbed metals on laboratory time scales (Jenne, 1968; Rose and Bianchi-Mosquera, 1993), but release could occur if precipitates are dehydrated and become more crystalline. If a poorly crystalline precipitate transforms to more crystalline

goethite or even hematite, metals can be excluded from the new structure due to a decrease in crystal lattice space and/or a decrease in surface area on which sorption reactions can occur.

In addition to crystallinity, the aggregation of particles could also control the sorption and desorption of trace metals. Aggregation decreases the surface area available for sorption and can also prevent trace metal release as surfaces once exposed are no longer open to the surrounding solution (Coughlin and Stone, 1995).

5.4. Influence of dissolved species on metal sorption

5.4.1. Sodium

The presence of elevated concentrations of sodium in solution could enhance anion sorption due to the effect of the ionic strength of the solution. Sorption of cations onto the iron hydroxide surface can be specific or nonspecific. Specific adsorption leads to the formation of inner-sphere complexes in which the element is coordinated to one or two surface Fe atoms; most heavy metal and alkaline earth cations sorb in this manner (Cornell and Schwertmann, 1996). Nonspecific adsorption, exhibited by alkali metals (e.g. sodium), involves ion pair formation and the formation of outer-sphere complexes. The ion is surrounded by water molecules and held to the surface by electrostatic conditions (Collins et al., 1999) and depends on ionic strength of the solution, which influences electrostatic conditions at the surface (Cornell and Schwertmann, 1996).

When present at low levels in the water (<100 mg/L), dissolved sodium has a nominal effect on the iron hydroxide surface. However, the high Na concentrations at the Scrubgrass (293 mg/L) and P-A (790 mg/L) sites result in a significant increase in the positive surface charge. This in turn enhances anion sorption and can explain the elevated As concentrations seen in the

first precipitates forming in the two systems. As the pH_{pzc} is approached, the effect of ionic strength could decrease as competition from other sorbing cations (with higher affinities for the oxide surface) increases.

5.4.2. Sulfate

Dissolved sulfate in the discharges could influence the sorption of Zn, Cu, Pb and Cd onto the precipitates by creating a net negative charge at the iron hydroxide surface (e.g., Balistrieri and Murray, 1982; Ali and Dzombak, 1996b). Alternatively, sulfate can form ternary structures (Schindler, 1990; Ali and Dzombak, 1996b; Webster et al., 1998) with the trace metal cations of Co, Mn, Ni and Zn, creating a mixed metal-ligand surface complex that increases the amount of metal cations associated with the iron hydroxides.

Either process (electrostatic alteration or formation of ternary complexes) could be operating in the mine drainage treatment system, as sulfate is ubiquitous in many discharges. Other anions present in CMD, such as carbonate and bicarbonate, can also act in a manner similar to sulfate (Balistrieri and Murray, 1982).

5.4.3. Manganese and iron

The presence of a particular trace metal in solution does not necessarily reflect what will sorb and accumulate in the precipitate. The presence of other dissolved constituents may hinder sorption and subsequent incorporation into the goethite structure. The dissolved Mn concentration in water at the Howe Bridge site is an order of magnitude higher than at the Elklick site, but the concentration of Mn in the Elklick precipitates is up to 15 times higher then

that at the Howe Bridge site (Figure 10a). A combination of two processes can be used to explain this. In the first, ferrous inhibits Mn^{2+} oxidation, and in the second ferric acts to oxidize Mn^{2+}.

Following sorption, Mn must be oxidized from Mn^{2+} to Mn^{3+} before it can be incorporated into the goethite structure and allow continued surface sorption to occur (Giovanoli and Cornell, 1992). In passive treatment systems Mn^{2+}, the most common form of Mn in natural waters (Hem, 1992), can be oxidized and removed only after the oxidation and removal of Fe^{2+}. This typically does not happen abiotically at pH < 9.0, as the kinetics of this reaction are low; once Mn is oxidized, it is immediately reduced by the Fe^{2+} (Hedin et al., 1994). Figure 10b shows that the concentration of dissolved Fe is about four to five times less at Elklick than at Howe Bridge. The majority of total dissolved Fe throughout Howe Bridge and Elklick is in the Fe^{2+} form, except for location 3 at Elklick, which is mostly Fe^{3+} (Table 1).

It is reasonable to assume that continued sorption of Mn to the precipitates at the Howe Bridge site is limited by the incorporation of Mn into the goethite structure. Incorporation cannot occur until Mn is oxidized, but at Howe Bridge it is inhibited by the presence of high amounts of dissolved Fe^{2+} (up to 247 mg/L) found in most of the system. At Elklick, however, Fe^{2+} concentrations decrease from 51 mg/L to 6.5 mg/L between Locations 1 and 3, and sorption of Mn and subsequent oxidation and incorporation into the goethite structure can occur, accounting for the high Mn in the precipitate at Elklick.

Alternatively, at low concentrations of dissolved Fe, a catalytic mechanism can result in the oxidation of Mn^{2+} by Fe^{3+} (Hem, 1964; Hem, 1977):

$$2Fe(OH)_2^+ + 3Mn^{2+} + 2H_2O \rightarrow Mn_3O_4 + 2FeOH^+ + 6H^+$$

The reaction proceeds to the right at a pH > 6.5, when dissolved Fe^{2+} activity is low (concentrations of 10^{-12} molal; Hem, 1977; Cravotta, 1999). Cravotta and Trehan (1999) used this mechanism to explain the removal of dissolved Mn in oxic limestone drains built to treat drainage from coal mines. It is feasible that this process could also be operating in the Elklick system (Figure 10).

Regardless of the mechanism by which Mn can oxidize and precipitate on the goethite surface, it is possible that the presence of Mn oxide or hydroxide phases could enhance the sorption of other metals such as Co, Ni and Zn. As stated earlier, these metals have an increased affinity at Elklick (Elklick CR values are ~1.5 times greater than those of the Howe Bridge system). This could be due to the presence of Mn oxide and/or hydroxide phases on the goethite surface at the Elklick site. Hydrous Mn oxides are known to have higher sorption capacities compared to the iron hydroxides, especially for Co and Ni (Manceau et al., 2000; Trivedi and Axe, 2000; Trivedi et al., 2001). Thus, it is necessary to identify the phases in treatment system precipitates (e.g., goethite, manganese hydroxides, and organic matter) that are actually associated with trace metals of interest.

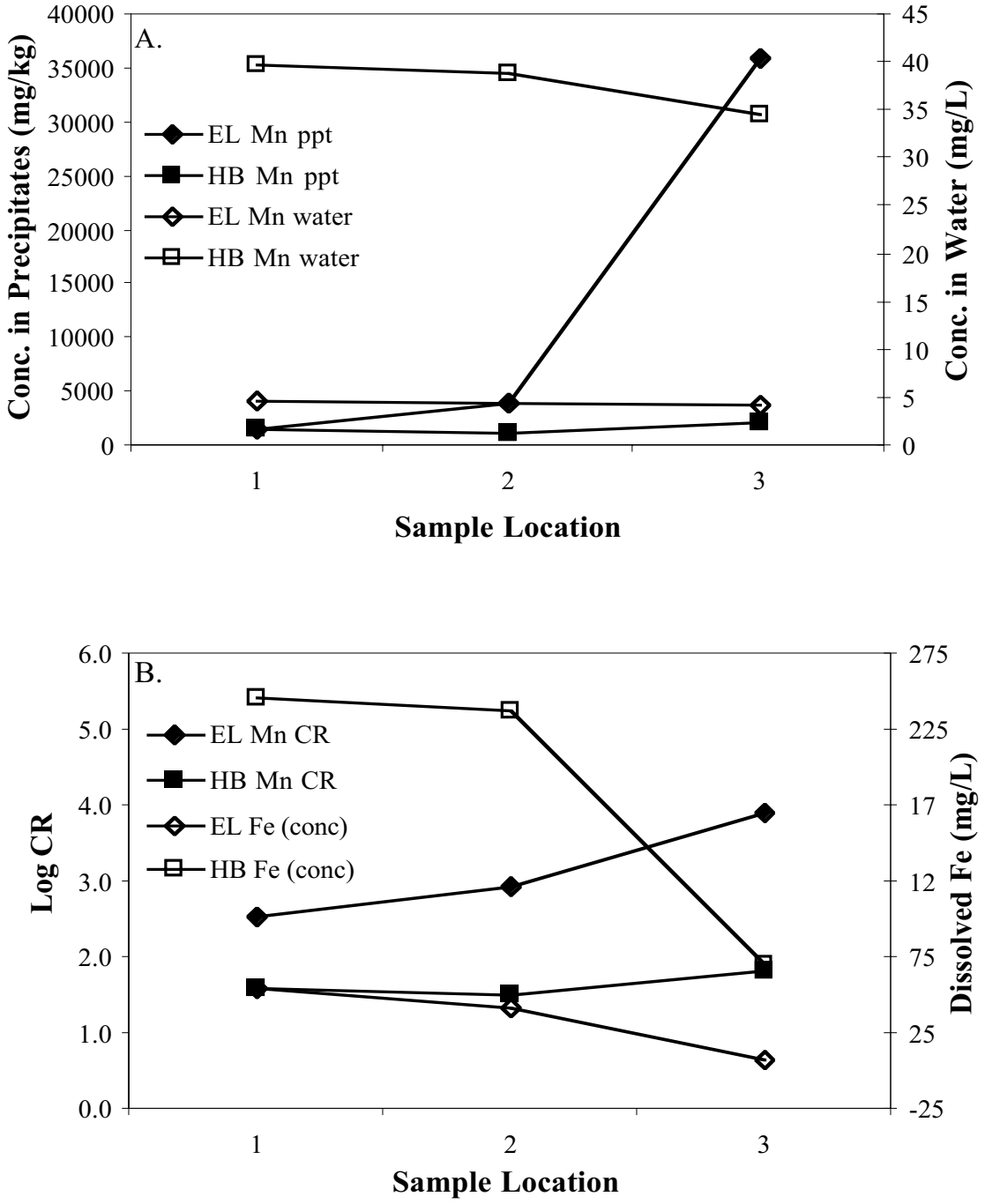

Figure 10. (a) Manganese concentration in the precipitates and water collected from Howe Bridge and Elklick; (b) Manganese concentration ratios and dissolved iron for Howe Bridge and Elklick.

5.5. Sequential extraction and trace element associations

In order to determine how metals are associated with the precipitates, a sequential extraction procedure was developed. This five step procedure is a modification of a combination of procedures (Tessier et al., 1979; Lovley and Phillips, 1987; Schwertmann and Cornell, 1991; Ure et al., 1993; McCarty et al., 1998) and a detailed discussion on method development and results is presented in Chapter 2, though it is necessary to discuss some of the results here. The procedure targeted metals loosely sorbed (Milli Q) and tightly sorbed (0.1 M acetic acid) to the iron hydroxide surface, bound to manganese oxides and hydroxides (0.1 M hydroxylamine hydrochloride), bound to iron oxides and hydroxides (0.25 M hydroxylamine hydrochloride) and bound to organic matter and sulfides (hydrogen peroxide and 1 M ammonium acetate).

Results of the extraction method for a sample from the Morrison site are presented in Figure 11a, and are representative of the results seen in most of the other samples used in that study (see Chapter 2). This figure shows that the trace metals (including manganese) are released in the step targeting the iron oxide and hydroxide phase, indicating they are tightly bound or incorporated into the goethite structure. Transition metals are specifically sorbed to the iron hydroxide surface and reversal of this is difficult (Cornell and Schwertmann, 1996), which is why sorbed metals are not exchanged with the acetic acid step. However, in one sample from the Elklick system (EL-3, Figure 11b), the majority of the Mn (35,000 mg/kg, about 97% of the total extractable Mn) was released during the 0.1 M hydroxylamine hydrochloride extraction step, indicating the presence of Mn oxide or hydroxide phases. Due to the amorphous nature of this sample, it could not be determined by XRD if such phases were present. The majority of Co was released in this step, indicating that it was sorbed or incorporated into the Mn

oxide/hydroxide structure, and therefore had a higher affinity for manganese hydroxides than for iron hydroxides. Nickel was partitioned between the Mn and Fe oxide/hydroxide phases, as was Zn, though Zn was more strongly partitioned into the iron hydroxide phase. These results indicate that the majority of trace metals are incorporated into the iron oxide/hydroxide phase (or will partition into a manganese oxide/hydroxide phase if present), and they are not easily desorbed/released. This implies that CMD precipitates could have the ability to continually uptake metals and prevent them from being released back into the aquatic environment.

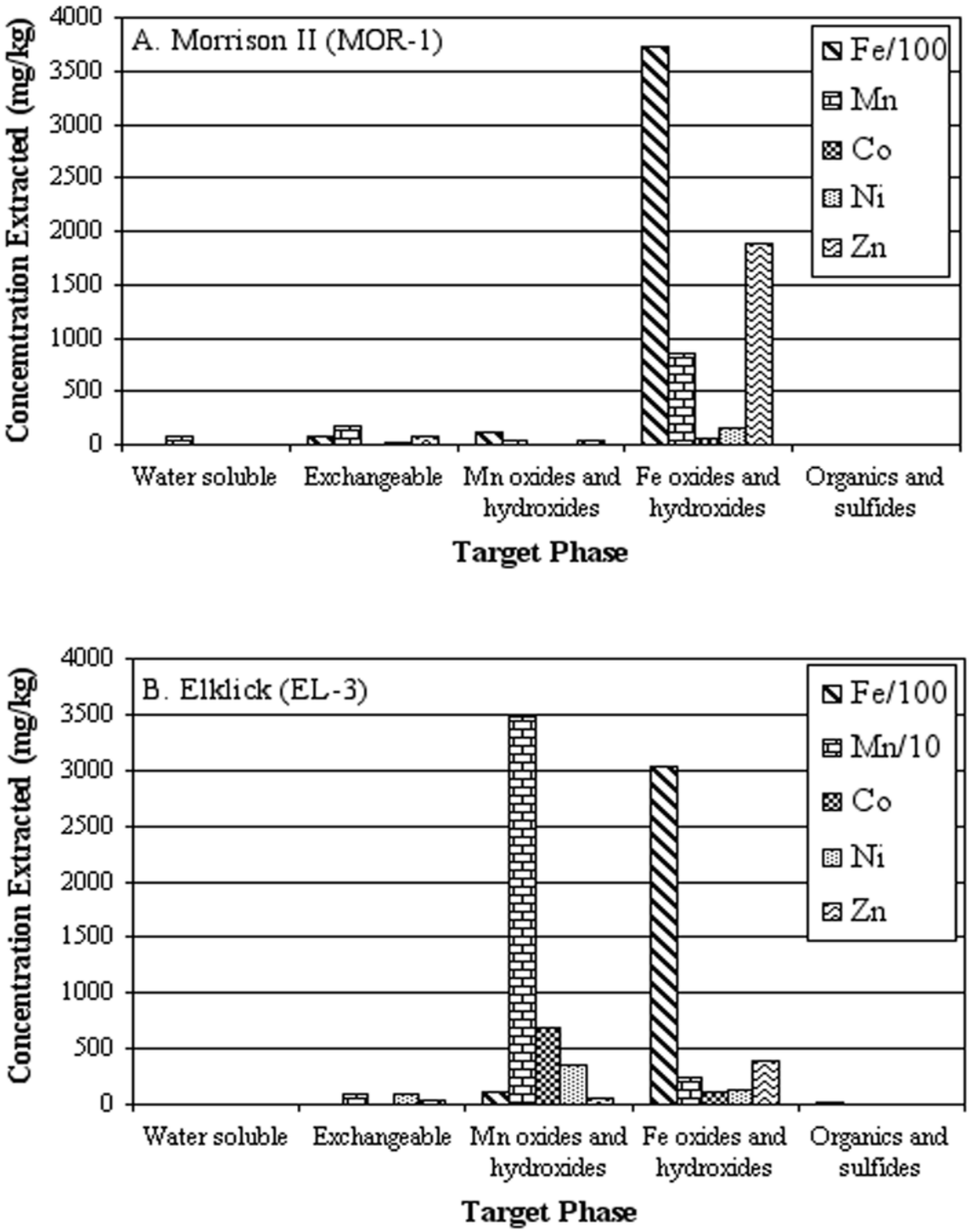

Figure 11. Results of sequential extraction procedure: (a) Morrison II, sample MOR-1; (b) Elklick, sample EL-3.

5.6. Influence of coal seam and overburden on precipitate chemistry

Postmining water quality depends on the coal seam from which a discharge originates as well as the overburden of that coal seam. Mining exposes minerals in the overburden such as pyrite to weathering processes, which result in the formation of mine drainage. A number of tools, such as acid base accounting, can be used for the prediction of postmining water quality (Brady et al., 1998). In a similar manner, it might be possible to predict the trace metal constituents that could accumulate in the precipitates that form based on the water quality of the discharges.

It is generally believed that coal is deposited in freshwater environments. Deposition of overburden strata can occur in freshwater, transitional (brackish) or marine environments, and the overburden depositional environment partially dictates the authigenic and diagenetic minerals that form in coal and its associated strata (Brady et al., 1998). Strata deposited under marine and brackish conditions are typically high in sulfur due to sulfate in the seawater. Higher concentrations of manganese are also associated with marine and brackish strata.

These trends are reflected in the water quality data from this study. High sulfate (up to ~1300 mg/L) and manganese (up to 41 mg/L) are seen in discharges originating from the Clarion seam, which is overlain by marine units. In marginally brackish environments (overburden of Kittanning and Freeport coals, Elklick and P-A discharges), the sulfur and manganese contents will be a function of the extent of marine influence, and in freshwater environments (Pittsburgh coal, Scrubgrass discharge), the sulfur and manganese contents should be considerably lower than coal seams overlain by marine units.

Sulfate, sodium and ferrous iron concentrations can all influence the sorption of trace metals to the iron hydroxide surface. In order to accurately predict the type of precipitate that will form

from a given discharge, factors that can influence discharge geochemistry, such as overburden geology, should be considered. The pH of the water, which is also a function of the strata it travels through (e.g., shales vs. alkalinity generating limestones), will also influence the type of iron hydroxide that forms as well as what trace metals are subsequently sorbed. Even though trace metals may be present at or below detection limits, they can still concentrate in the precipitate, especially if sorption is promoted by the presence of other dissolved constituents.

The type of mine (underground vs. surface) may also influence water quality. The Scrubgrass and P-A discharges both originate from underground coal mines, and the high levels of sodium seen in these discharges could be due to subsurface cation exchange reactions or reactions with brines (e.g., Winters et al., 1999; Capo et al., 2001).

6. Conclusions

Precipitates formed in five coal mine drainage passive treatment systems in southwestern Pennsylvania and northwestern Maryland are dominantly (> 70%) goethite; crystallinity varies throughout an individual system, and lower crystallinity is associated with enhanced sorption of trace metals. High surface area and cation vacancies within the goethite structure enable sorption and incorporation of metals from CMD polluted waters. Sorption affinities (determined by the log of the concentration ratio) follow the order of Al>Zn>Co≈Ni>Mn and are consistent with those determined experimentally and on synthetic goethite. Cobalt, Ni and Zn are preferentially sorbed to Mn oxide phases when present.

As pH increases in the individual CMD treatment systems toward the pH_{pzc}, arsenic sorption decreases and Al and transition metal (Co, Mn, Ni, and Zn) sorption increases. In the Morrison II system, arsenic sorption also decreases with increasing pH, but there is no corresponding

increase in transition metal cation sorption as the pH_{pzc} is approached. This could be due in part to higher crystallinity within the Morrison II system relative to the other CMD systems, which inhibits trace metal cation sorption processes. Aluminum enrichment and the high affinity of aluminum for the goethite surface, particularly at the Morrison II site, could also be a result of isomorphous substitution.

Discharge water chemistry can have a strong effect on metal sorption. Dissolved Na present at levels > 100 mg/L increases the ionic strength of the waters and could increase the positive charge at the surface of the precipitates, resulting in enhanced sorption of anions such as those of arsenic. Dissolved sulfate could also change electrostatic conditions at the surface by making it more negative and enhancing trace metal cation sorption (e.g., Co, Mn, Ni and Zn). It is also possible that sulfate could form ternary complexes with these cations.

Even though dissolved Mn concentrations at Howe Bridge are 10 times higher than that at Elklick, the concentrations of Mn in the precipitates at Elklick are about 15 times higher than at Howe Bridge, showing that dissolved elemental concentrations do not necessarily reflect what ultimately accumulates in the precipitate. Sorption and incorporation of Mn are limited by oxidation processes, which are limited by the presence of ferrous iron in solution.

Results of this study have implications not only for disposal of precipitates but also for the optimization of passive treatment systems. Degree of crystallinity (and subsequently morphology and trace metal associations) are a function of the treatment system and how rapidly ferrous iron is oxidized, forms precipitates, aggregates and settles. Precipitates formed earlier in the passive treatment systems tend to have the highest crystallinity and the lowest concentrations of trace metal cations.

In order to optimize passive treatment systems for resource recovery purposes, net-alkaline waters (whether naturally so or made alkaline through the use of an ALD) should undergo intense oxidation as soon as possible and be allowed to precipitate and settle in large, unvegetated ponds early in the system. Increased oxidation could enhance the crystallinity of the precipitate, as seen in Morrison II. Precipitates formed after this point are likely to be less crystalline and have greater enrichment of Al, Co, Mn, Ni and Zn. Jeon (1998) found that the greater the crystallinity exhibited by the precipitate, the smaller the settling volume of the precipitate. A more crystalline precipitate will not only be cleaner, it will also occupy less space in treatment ponds, potentially extending the life of the system.

Even though a metal is present in solution, its concentration is not necessarily an accurate predictor of what metals accumulate in the precipitate. Goethite crystallinity, pH of the associated water, trace metal affinities and the presence of dissolved sodium and sulfate all affect metal sorption to CMD precipitates. Further research is needed to constrain the parameters influencing coal mine drainage precipitate characteristics in order to develop a predictive model for precipitate formation.

Chapter 2

Development of a Sequential Extraction Procedure for Mine Drainage Precipitates

1. Introduction

Numerous processes control the fate and transport of heavy metals in polluted waters and soils, including: (1) ion exchange (nonspecific adsorption), (2) surface complexation (specific/chemical adsorption to surface hydroxyl groups or metal hydroxides), (3) coprecipitation (solid solution/isomorphous substitution or mechanical enclosure of the metal containing solution), and (4) organic complexation (Butler, 1964; Walton, 1979; Karthikeyan et al., 1997; Martínez and McBride, 1998). Fe hydroxides, such as goethite (∝-FeOOH) and ferrihydrite (Fe_5HO_8-$4H_2O$), are known for their ability to sorb (and subsequently incorporate into the crystal structure) potentially toxic trace metals from the environment, thereby playing an important role in their mobility and transport, especially in mine drainage contaminated waters (Karlsson et al., 1988; Blowes and Jambor, 1990; Tarutis and Unz, 1994; Herbert, 1996). A number of laboratory studies examine the sorptive abilities of iron oxides and hydroxides in detail (Jenne, 1968; Benjamin and Leckie, 1980; Pierce and Moore, 1980; Balistrieri and Murray, 1982; Esmadi and Simm, 1995; Trivedi and Axe, 2000).

Single (Lindsay and Norvell, 1978; Beckett, 1989) and sequential (Tessier et al., 1979; Saeki and Matzumoto, 1994; Gómez-Ariza et al., 1999; Keon et al., 2001; Wenzel et al., 2001) chemical extraction procedures have been developed and used to evaluate the mobility and availability of potentially toxic trace elements for sediments and soils. The majority of trace element studies on mine drainage precipitates have been carried out on iron oxide precipitates from acidic “hard rock” mining discharges (e.g., metal mines from massive sulfide, crystalline

felsic rock and skarn deposits). Karathanasis and Thompson (1995) and Herbert (1996) used single extraction schemes to evaluate iron content and total metals content of mine drainage precipitates, respectively. McCarty et al. (1998) evaluated numerous extractants designed to dissolve poorly crystalline and crystalline iron hydroxide precipitates.

Recent research shows that the Fe hydroxide precipitates formed from bicarbonate buffered bituminous coal mine drainage (CMD) waters are comprised mainly of goethite (>85%), and are enriched in certain trace elements, including As, Co, Mn, Ni, S and Zn (Kairies et al., 2000). It is evident that coal mine drainage precipitates play a role in the mobility and availability of trace elements in streams that receive the related discharges. However, no sequential extraction procedure exists to determine how trace metals are associated with these Fe hydroxide precipitates. Total metals analyses provide only limited insight.

One commonly used sequential extraction procedure is a three step method developed by the Standards, Methods and Testing (SM&T) Programme of the European Commission in the 1990s in an effort to standardize extraction schemes (Ure et al., 1993). This procedure has been successfully used to look at metal partitioning in river, lagoon, intertidal and lake sediments (Martin et al., 1998; Mester et al., 1998; Gómez-Ariza et al., 2000; Tokalioglu et al., 2000) and contaminated soils (Maiz et al., 1997; Davidson et al., 1998). However, some researchers have found that the 0.1M hydroxylamine hydrochloride step (Step Two of the SM&T method) intended to target both Mn and Fe oxides and hydroxides does not effectively dissolve Fe oxides (Whalley and Grant, 1994). In 1999, the method was modified by replacing this step with a 0.5 M hydroxylamine hydrochloride (in 0.05 M HNO_3) extraction step (Rauret et al., 1999) and was successfully used to examine metal partitioning in road sediment (Sutherland, 2002) and certified reference materials (Sahuquillo et al., 1999; Sutherland and Tack, 2002). However, this

modified method does not separate metals bound to Fe oxides and hydroxides from Mn oxide and hydroxide bound metals. Additionally, as with most sequential extractions, the SM&T method only addresses partitioning of divalent metals, not anions (Keon et al., 2001; Wenzel et al., 2001).

Some shortcomings associated with sequential extraction procedures include the poor selectivity of extractants (Tipping et al., 1985; Kheboian and Bauer, 1987), potential alteration of the material being extracted (Keon et al., 2001) and post extraction readsorption (Kheboian and Bauer, 1987; Raksasataya et al., 1996), which can lead to an overestimation of metals associated with the residual phase (Gómez-Ariza et al., 1999). Although some researchers criticize sequential extraction procedures (SEPs) (Kheboian and Bauer, 1987; Nirel and Morel, 1990; McCarty et al., 1998), they can be used to provide important information on trace element associations by defining operational phases or geochemical reservoirs (as is done in the SM&T procedure), such as "exchangeable" or "Fe oxide bound" (Raksasataya et al., 1996; Quevauviller et al., 1997). The mobility of trace metals, and the ease at which they are extracted from coal mine drainage precipitates, have implications for disposal as well as trace metal recovery.

The goal of this study was to develop a sequential extraction method to determine trace element (both cationic and anionic) associations on iron hydroxides formed form coal mine drainage. Two separate methods were developed: one involves a modification of the original SM&T procedure: the other incorporates anion exchange steps and uses acid ammonium oxalate to target the iron hydroxide phases.

2. Experimental

2.1. Sample collection and characterization

Iron hydroxide precipitate samples were collected from treated and untreated coal mine discharges in the bituminous region of eastern Pennsylvania and northwestern Maryland. Major and trace element analysis on bulk precipitates were determined by Activation Laboratories, Ontario, using instrumental neutron activation analysis (INAA) and total acid digestion followed by analysis using inductively coupled plasma atomic emission spectroscopy (ICP-AES). Based on these results (Table 4), five representative samples, including samples with elevated levels of As (SG-0601-1), Ni (EL-3), Zn (MOR-1), and Mn (EL-1), were selected to undergo the sequential extraction procedures.

2.2. Reagents

All reagents were trace metal grade or certified A.C.S. Milli-Q® water (MQW, 18 MΩ•cm) was used to make up all extractants, as well as for the water rinse step of the procedure. All HDPE plasticware used for reagent solutions and sample leachates were cleaned with 30% HNO_3 (soaking overnight). The PTFE centrifuge tubes were cleaned using 50% HCl, 50% HNO_3, 50% HCl, (eight hours for each step), followed by rinsing in MQW.

Table 4. Total elemental concentration (mg/kg) of precipitates used in the extraction.

Sample	Fe	Mn	As	Co	Ni	Zn	S
MOR-1	490000	1216	119	92	189	2400	7700
EL-1	536000	1645	11	68	70	202	3530
EL-3	420000	35928	6	936	698	757	2090
HB-2	571000	1294	19	25	29	405	11300
SG-0601-1	417000	252	1320	8	18	95	4680

2.3. Procedures

2.3.1. Sample pre-treatment

A Teflon® spatula was used to transfer approximately 15 – 20 grams of raw precipitate sample into 50 mL HDPE centrifuge tubes. All samples were centrifuged in an International Clinical centrifuge (model CL) to remove water. One gram of each centrifuged sample was used for the sequential extraction procedure. Samples were not dried or heated in order to avoid desiccation or thermally-related changes in trace element associations. A separate, equivalent amount of each sample was dried to determine a dry weight for use in calculations.

2.3.2. Sequential extraction

Two different methods were initially applied to the mine drainage precipitate samples. The first method incorporated anion exchange steps using $(NH_4)_2SO_4$ and NaH_2SO_4 for loosely and tightly sorbed As, respectively (as described in Keon et al., 2001 and Wenzel et al., 2001), and an ammonium oxalate reagent to target the Fe hydroxide phases. This method was tested and deemed inappropriate for two reasons: arsenic (which can be present as an oxyanion) was not detected in the anion exchange steps (possibly due to readsorption onto the sample), and only minor amounts of the Fe hydroxide precipitate were dissolved by the acid ammonium oxalate.

For the second method, the original SM&T procedure was modified by adding two steps (Table 5). A water rinse, added prior to the main extraction steps, targeted water soluble elements. Due to the poor selectivity of the 0.1 M hydroxylamine hydrochloride for the Fe hydroxide phases, an additional step using 0.25 M hydroxylamine hydrochloride (as in Lovely and Phillips, 1987) was incorporated into the procedure. The rinses between steps were also

modified; instead of using water, the respective reagent from each step was used for the subsequent rinse.

The modified SM&T procedure (Table 5) is described below:

Step One: 40 mL of MQW was added to 1 g of centrifuged precipitate in a 60 mL PTFE centrifuge tube. The tube was shaken for 15 min using a Burrell wrist-action shaker (model BB). The extractant was separated from the residue by centrifugation (at least 20 minutes) and pipetted into a 125 mL HDPE bottle, taking care not to pipette any of the residue. The bottle was tightly capped and retained for analysis at 4°C.

Step Two: 40 ml of 0.11 M acetic acid was added to the residue from Step One. The tube was shaken for 16 h, and the extractant was centrifuged and pipetted as described in Step One. The residue was then washed by adding 20 mL 0.11 M acetic acid, and shaking for 10 min. The rinse was separated from the residue by centrifugation and pipetted into the same 125 mL bottle. The bottle was tightly capped and retained for analysis.

Step Three: 40 mL of 0.1 M hydroxylamine hydrochloride was added to the residue from Step Two, and the extraction was performed as in Step Two, except 0.1 M hydroxylamine hydrochloride was used for the rinse step.

Step Four: 40 mL of 0.25 M hydroxylamine hydrochloride in 0.25 M HCl was added to the residue from Step Three and the extraction was performed as in Step Two, except the tubes were heated in a water bath at 85˚C for 16 h and 0.25 M hydroxylamine hydrochloride in 0.25 M HCl was used for the rinse step.

Step Five: 10 mL of hydrogen peroxide was added to the residue from Step Four in small aliquots to avoid violent reaction, and the tube was covered with a watch glass and left to digest for 1 h at room temperature with periodic manual shaking. The digestion was continued by

heating in a water bath at 85˚C for 1 h., then the cover was removed and heating continued until the volume was reduced to > 1 mL. An additional 10 mL aliquot was added to the residue and heated again in a water bath at 85˚C for 1 h., then the glass was removed and the volume was reduced to > 1 mL. After cooling to room temperature, 50 mL of 1 M ammonium acetate was added to the residue and the extraction was performed as in Step Two, except 25 mL of 1 M ammonium acetate was used for the rinse step.

A procedural blank was carried out using the same steps. It should be noted that it was difficult to completely centrifuge and settle all the particles (due to their colloidal nature) during Steps One and Two of the method. Extra care was taken to help prevent this material from being pipetted with the extracting solution.

Table 5. Sequential extraction procedure for coal mine drainage precipitates.

Step	Reagent	Nominal geochemical phase
1	MQW	Water soluble
2	0.11 M acetic acid	Carbonates, exchangeable metals
3	0.1 M hydroxylamine hydrochloride (pH=2)	Mn oxides and hydroxides
4	0.25 M hydroxylamine hydrochloride in 0.25 M HCl	Fe oxides and hydroxides
5	8.8 M hydrogen peroxide; 1M ammonium acetate (pH=2)	Organic matter and sulfides

2.3.3. Metals analysis

Trace and major elemental composition of the extracting solutions were determined using inductively coupled plasma atomic emission spectroscopy (ICP-AES). Analyses were conducted at the University of Pittsburgh (UP) and at the U.S. Department of Energy National Energy Technology Laboratory (U.S. DOE NETL) on an axial Spectro-Flame end-on plasma instrument and an ICP-AES Perkin-Elmer Optima 3000, respectively. Wavelengths used for each element are listed in Table 6. Matrix interferences were corrected for by (1) scanning the various matrix blanks and standard solutions in the matrices and setting background positions with respect to the different matrix effects (UP) or (2) using a deconvolution program to model and correct the matrix effects of each extracting solution (U.S. DOE NETL). Standard samples were prepared and analyzed at each lab to enable interlaboratory comparison. QA/QC protocol followed EPA Method 6010 for ICP analysis of inorganic species.

Table 6. Wavelengths (nm) used for ICP-AES analysis.

Element	Spectro-Flame	Perkin Elmer Optima 3000
Fe	259.940	238.204
Mn	257.610	257.610
As	189.979	188.979
Co	228.616	228.616
Ni	231.604	231.604
Zn	213.856	206.200
S	182.040	180.669

3. Results and Discussion

3.1. Method recoveries

In order to determine how effective the method was for extracting metals, a total percent recovery value was calculated. For each element, the total concentration obtained from bulk analysis for a given sample (Table 4) was compared to the total concentration extracted by the method (Tables 7a-g) as follows:

Total Recovery (%) = [(Total of all extraction steps)/Bulk total]*100

The recoveries (Tables 7a-g) are generally within 80 – 120%. Recoveries greater or less than 100% could result from different factors. First, low (<80%) recoveries could arise when low concentrations (<10 mg/kg) of a particular element in the sample are present, as even a small (1 or 2 mg/kg) difference between the amount in the bulk sample and that actually extracted yields a higher relative error compared to other samples with higher concentrations of that particular element (e.g., in SG-0601-1, 5 mg/kg out of 8 mg/kg (difference of 3 mg/kg) of Co were extracted, giving a 62% recovery, while in EL-3 806 mg/kg out of 936 mg/kg (difference of 130 mg/kg) of Co were extracted, giving an 86% recovery). Agreement between the duplicate samples (MOR-1 and MOR-1 DUP; EL-3 and EL-3 DUP) in this study for % recoveries was good (within +/- 15%).

Recoveries will be affected if insoluble material remains following the extraction method, as metals are potentially incorporated into this fraction. Iron stained residue remained in MOR-1, MOR-1 DUP, HB-2 and SG-0601-1 after the sequential extraction was complete. However, subsequent analysis by X-ray diffraction methods (XRD) showed the material was predominantly (>90%) quartz. The presence of some visible Fe indicates incomplete dissolution during Step Four, which targeted the iron oxides and hydroxides. These results suggest that to

ensure total dissolution of Fe oxides and hydroxides and to improve metal recovery in Step Four, samples with high Fe concentrations (>40,0000 mg/kg) could require an increase in the volume of the extracting solution (0.25 M hydroxylamine hydrochloride in 0.25 M HCl). A final aqua regia and HF digestion step added to target any residual phase could also potentially improve recovery values.

Finally, a certified reference material would have aided in determining sources of variability of the recoveries (either in total metal analysis or in the extraction scheme), though no material comparable the precipitates examined in this study could be found.

Table 7. Sequential extraction results.

(a) Sequential extraction results for Fe (mg/kg)

Sample	Step 1	Step 2	Step 3	Step 4	Step 5	Sum	% Recovery
MOR-1	209	7189	11889	373333	72	392692	80.1
MOR-1 Dup	142	9115	17204	367587	554	394602	80.5
EL-1	42.7	21598	8997	322546	118	353301	65.9
EL-3	100	563	10520	303277	1722	316182	75.3
EL-3 Dup	136	694	10493	287076	1347	299746	71.4
HB-2	123	1577	2932	448598	219	453448	79.4
SG-0601-1	288	6958	8047	230853	598	246744	59.2

nd = not detected; detection limit = 0.001 mg/L

(b) Sequential extraction results for Mn (mg/kg)

Sample	Step 1	Step 2	Step 3	Step 4	Step 5	Sum	% Recovery
MOR-1	85.5	169	47.0	858	nd	1159	95.4
MOR-1 Dup	86.1	149	37.0	668	nd	940	77.3
EL-1	27.7	374	42.7	694	nd	1138	69.2
EL-3	1.89	941	34882	2341	12.9	38179	106.3
EL-3 Dup	2.87	917	30467	2368	10.0	33766	94.0
HB-2	165	11.8	7.04	555	nd	739	57.1
SG-0601-1	nd	64.7	18.6	79	nd	163	64.8

nd = not detected; detection limit = 0.002 mg/L

(c) Sequential extraction results for S (mg/kg)

Sample	Step 1	Step 2	Step 3	Step 4	Step 5	Sum	% Recovery
MOR-1	821	214	385	5318	nd	6738	87.5
MOR-1 Dup	950	266	471	5233	nd	6919	89.9
EL-1	760	46.7	73.2	593	nd	1473	41.7
EL-3	685	16.3	371	882	nd	1955	93.5
EL-3 Dup	654	13.4	209	768	nd	1644	78.7
HB-2	1015	459	552	7559	nd	9584	84.8
SG-0601-1	668	34.1	2167	808	221	3897	83.3

nd = not detected; detection limit = 0.020 mg/L

Table 7 (continued)

(d) Sequential extraction results for As (mg/kg)

Sample	Step 1	Step 2	Step 3	Step 4	Step 5	Sum	% Recovery
MOR-1	1.16	7.29	4.70	101	nd	114	95.9
MOR-1 Dup	nd	7.86	6.32	98.4	nd	113	94.6
EL-1	1.08	4.74	1.47	0.76	nd	8.04	76.5
EL-3	nd	2.40	3.18	nd	nd	5.58	97.8
EL-3 Dup	nd	2.45	4.19	nd	nd	6.64	117
HB-2	1.31	3.29	nd	4.04	nd	8.63	46.4
SG-0601-1	2.38	32.5	6.72	785	nd	827	62.6

nd = not detected; detection limit = 0.020 mg/L

(e) Sequential extraction results for Co (mg/kg)

Sample	Step 1	Step 2	Step 3	Step 4	Step 5	Sum	% Recovery
MOR-1	nd	5.54	2.26	67.4	nd	75.7	82.3
MOR-1 Dup	nd	5.60	2.41	77.2	nd	85.6	93.0
EL-1	nd	8.73	2.84	55.7	nd	67.2	98.9
EL-3	nd	6.40	690	108	1	806	86.1
EL-3 Dup	nd	6.27	548	98.6	nd	653	69.8
HB-2	2.92	nd	nd	19.7	nd	22.7	90.6
SG-0601-1	nd	2.28	nd	2.69	nd	4.97	62.1

nd = not detected; detection limit = 0.005 mg/L

(f) Sequential extraction results for Ni (mg/kg)

Sample	Step 1	Step 2	Step 3	Step 4	Step 5	Sum	% Recovery
MOR-1	2.02	14.9	9.13	162	nd	188	99.4
MOR-1 Dup	2.18	17.1	11.0	139	nd	169	89.5
EL-1	nd	10.1	5.46	67.4	nd	83.0	119
EL-3	nd	90.1	360	121	nd	571	81.9
EL-3 Dup	nd	85.4	414	117	nd	617	88.4
HB-2	7.48	1.68	2.50	19.9	nd	31.6	109
SG-0601-1	nd	5.50	4.08	8.29	nd	17.9	99.3

nd = not detected; detection limit = 0.005 mg/L

Table 7 (continued)
(g) Sequential extraction results for Zn (mg/kg)

Sample	Step 1	Step 2	Step 3	Step 4	Step 5	Sum	% Recovery
MOR-1	3.96	73.6	44.9	1879	0.92	2002	83.4
MOR-1 Dup	3.53	83.7	54.8	1795	2.76	1940	80.8
EL-1	nd	52.9	21.6	219	nd	294	145
EL-3	nd	45.3	61.2	388	2.36	497	65.6
EL-3 Dup	nd	43.6	53.9	355	1.77	454	60.0
HB-2	4.58	2.36	1.35	367	0.50	375	92.7
SG-0601-1	nd	9.34	9.9	60.3	0.94	80.5	84.7

nd = not detected; detection limit = 0.0015 mg/L

3.2. Trace element associations

Although metal recoveries are not equal to 100%, results from the extraction method can still provide useful information on how trace metals are associated with the Fe hydroxide precipitates. Extraction data are presented in Tables 7a – g. For each sample, less than 5% of the total extractable Fe was released in Steps One and Two (e.g., MOR-1, Figure 12a). The Fe in these two steps is likely colloidal particles that did not settle during centrifugation, though it could also indicate slight dissolution of the precipitate.

Step Four extracted 55 – 76% of the total Fe for all samples. With the exception of EL-3, between ten and twenty times more Co, Mn, Ni and Zn (Tables 7b, e-g) were also extracted in this step compared to other steps (e.g. MOR-1, Figure 12a), indicating the associated metals are potentially sorbed to the surface or are incorporated into the Fe hydroxide structure. Transition metals (e.g., Co, Mn, Ni, and Zn) form inner-sphere complexes through specific (chemical) sorption, and as a result, desorption from the surface is difficult (Cornell and Schwertmann, 1996). Once metals are sorbed to the Fe hydroxide surface, they tend to desolvate and become incorporated into the hydroxide crystal structure difficult (Cornell and Schwertmann, 1996). It follows that metals released during this step were probably sorbed to the surface and incorporated into the structure of the Fe hydroxide precipitates, and are not water soluble or easily exchangeable. These associations indicate that the mobility of Co, Mn, Ni and Zn is low and they will remain in association with the precipitate.

In sample EL-3 (Figure 12b), the majority (>70%) of the total extracted Fe is also released in Step Four. However, more than 97% of the total extracted Mn is released in Step Three, while less than 8% Mn was released from the other samples during this step (e.g., MOR-1, Figure 12a).

This indicates that Mn oxide/hydroxide phases are present in sample EL-3 and not in the other samples. In addition, compared to the other samples, five to six times more Co and three to four times more Ni is released in Step Three than in Step Four for sample EL-3. This suggests preferential partitioning of Co and Ni for the Mn oxide/hydroxide phases (when present) over the main iron hydroxide phase. Any remaining Mn in sample EL-3 is released in Step Four, indicating it is either sorbed to the surface or incorporated into the crystal structure of the Fe hydroxide, as with the other samples, and is not associated with the separate Mn oxide/hydroxide phase.

Arsenic from all samples is released in Steps Two, Three and Four (Table 7d), suggesting it is exchangeable and potentially bound to both Mn and Fe oxide/hydroxide phases. If As is easily exchanged, it is potentially available for reactions with the surrounding ecosystem.

For all samples, S was released in extraction Steps One through Four, as well as in Step Five for SG-0601-1 (Table 7c). It is possible that loosely sorbed S (probably present as sulfate) was released during Steps One and Two, some of which could have subsequently readsorbed to the remaining precipitate and been released in later extraction steps.

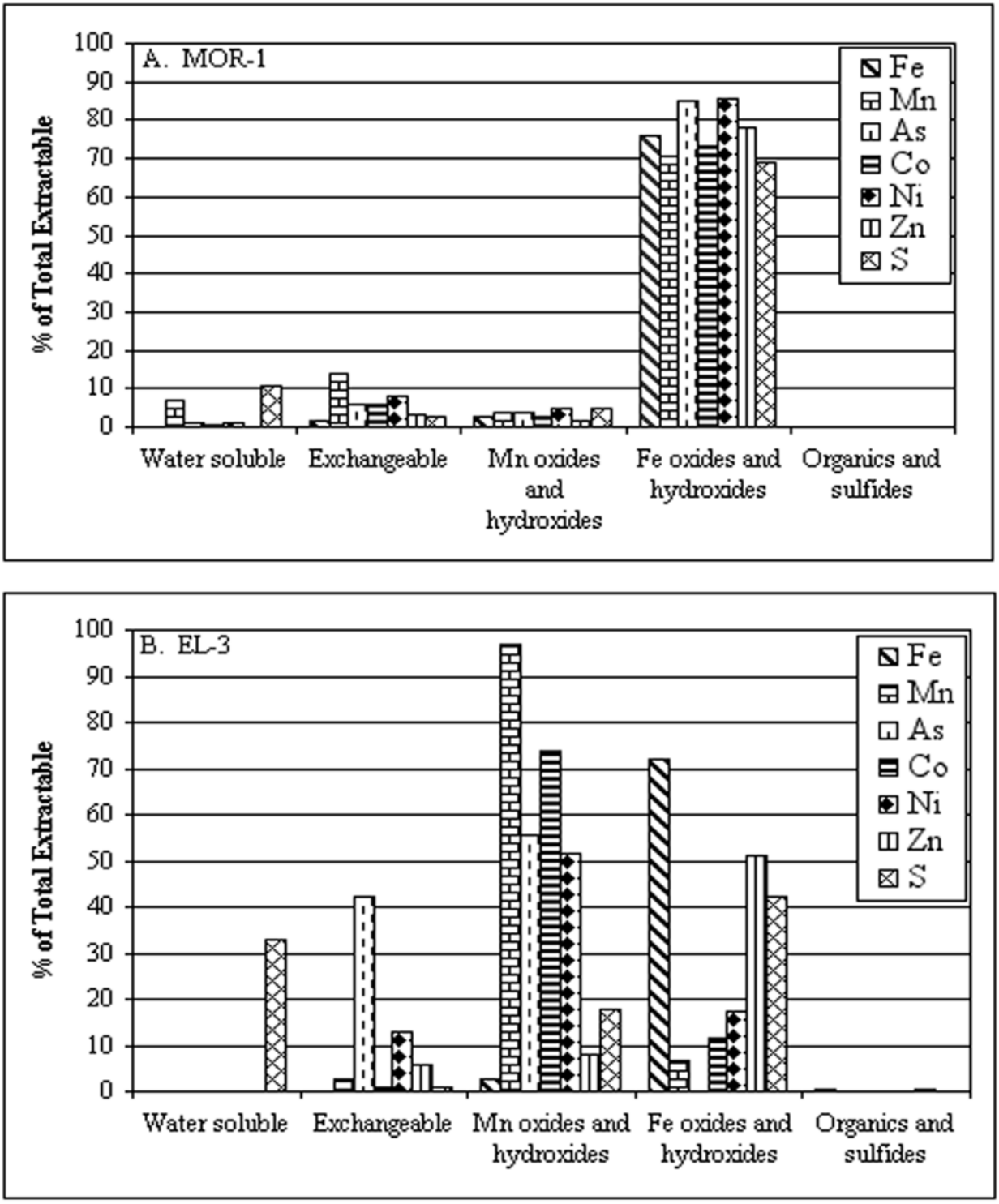

Figure 12. Percent of total extracted for individual metals released during each step. (a) MOR-1; (b) EL-3.

4. Conclusions

The modified SM&T procedure provides a successful way to evaluate partitioning of trace metals in precipitates formed from coal mine drainage by defining each extraction step as an individual geochemical reservoir. Single extraction and total digestion schemes cannot provide information on the types of metals associated with different phases and how they are partitioned, making it difficult to evaluate their potential mobility in and availability to the environment.

The results of this study indicate that trace metals (Co, Mn, Ni and Zn) are predominantly incorporated either into the lattice structure of the Fe hydroxide precipitate or tightly sorbed to the surface, and are not readily solubilized or exchanged. If a Mn oxide or hydroxide phase is present, Co and Ni will preferentially partition into this phase. The long term mobility of these elements is subsequently controlled by the stability of the Fe or Mn oxide/hydroxide precipitate; as long as the precipitate is not subjected to conditions that promote its dissolution or transformation, the associated trace metals will remain fairly immobile and unavailable to the aquatic ecosystem.

Iron hydroxides are excellent sorbents and concentrators of trace metals. Based on this study, Co, Mn, Ni and Zn are not readily extracted, so the recovery of the trace metals would entail the complete dissolution of the iron hydroxide phase.

It is suggested that the volume of the 0.25 M hydroxylamine hydrochloride be increased to at least 50 mL, due to the concentrations of Fe in this type of sample to potentially improve dissolution and recovery of the Fe and other associated metals. A final aqua regia and HF step would target any residual phase, also increasing recoveries. The use of a certified reference material would also help to evaluate potential sources of variability as well as the accuracy of the method.

Chapter 3

Resource Recovery Potential of Coal Mine Drainage Precipitates

1. Introduction

Coal mining activities can produce discharges (coal mine drainage or CMD) with high concentrations ($10^1 – 10^3$ ppm) of dissolved iron (Fe), aluminum (Al), manganese (Mn), and sulfates (SO_4^{2-}), as well as trace concentrations of arsenic (As), cobalt (Co), nickel (Ni) and zinc (Zn). Prior to 1984 when effluent limitations were placed on mine operators, many mined sites were abandoned and discharges left to pollute receiving streams. The precipitation of metals such as Fe and Al as oxides and hydroxides onto stream bottoms can be detrimental to aquatic communities. An estimated 100,000 tons of iron per year is added to thousands of miles of waterways in the United States alone (Hedin, 1998). Continued treatment of CMD can be costly, and as a result, many are left untreated (Hedin et al., 1994).

Depending on the chemistry of a discharge, various treatment methods have been developed to remediate mine drainage contaminated water. Active treatment methods require the continual addition of alkaline chemicals to raise the pH and precipitate metals, leading to ongoing operation and maintenance costs that can be in excess of $100,000 annually (Hedin, 1996b). Passive treatment of net-alkaline drainage typically consists of a series of ditches, ponds and aerobic wetlands that aerate and detain water allowing the iron to oxidize, precipitate and settle (Watzlaf et al., 2000). Alkalinity can be added to net-acidic waters through various methods, including limestone dissolution and sulfate reduction. Although design and installation costs for passive systems can be as much as $100,000 - $200,000 (and sufficient land must be available to accommodate these systems), savings in yearly operation and maintenance costs compared to active treatment methods can be realized after a year or two of operation (Hedin, 1996b).

Both active and passive systems accumulate large volumes of precipitates over time. In the case of passive systems, as ponds and wetlands fill up with iron-rich precipitates, their ability to treat the water decreases. The sludge must then be dredged and is typically disposed of in landfills. The recovery and sale of metals from these precipitates could offset CMD treatment costs, particularly those associated with long-term operation and maintenance. Many passive systems are reaching the ten-year operation mark, and within the next decade precipitate removal and disposal issues will need to be addressed.

The potential for recovering the metal and metal oxides from CMD sludge exists, provided a market is available and the precipitates are of comparable or superior quality to those used by industry. The iron oxide market in the United States is about 160,000,000 kg/yr., some of which is imported (Hedin, 1996b). Iron oxides are commonly used by industry as pigments, colorants, catalysts, sorbents for water and gas purification, and as additives to feeds and fertilizers (Cornell and Schwertmann, 1996). They are either mined from ore deposits, produced synthetically, or form as a by-product during steel making (Hedin, 1996a).

The iron content of the iron oxides used by industry is variable (25 – 95%), depending on the application. If the iron oxides are to be used as additives to cosmetics or food, limits on As (<3 ppm), Pb (<10 ppm) and Hg (<3 ppm) must be met (2000). The price of commercial iron oxide ranges from $0.11 to over $2.75 per kg ($100 to over $2500 per ton) (Hedin, 1998).

Iron oxides in some CMD sludge formed from bicarbonate-buffered waters (natural or through limestone addition) are comparable (in Fe content, mineralogy and certain pigmentary characteristics) to natural iron oxides currently mined and used by industry (Fish et al., 1996; Hedin, 1998; Kirby et al., 1999). Additionally, mine drainage precipitates can be enriched in certain trace elements, including As (up to 3000 mg/kg), Co (up to 1060 mg/kg), Mn (up to 3.6

dry wt.%), Ni (up to 700 mg/kg) and Zn (up to 2200 mg/kg) (Kairies et al., 2001; Kairies et al., 2002). However, the relationship between the purity of the iron oxides and color has not been determined and it is not known weather the trace metal content of CMD precipitates vary with time or distance from the discharge.

The objective of this study was to determine spatial and temporal variations in mineralogy, morphology, chemical composition and color between precipitates that accumulated in a shallow channel over a number of years and to evaluate the suitability of these precipitates for use as a resource. Results of this study have implications for coal mine drainage remediation, resource recovery projects and wetland sludge disposal.

2. Study Area and Site Description

The site is an abandoned underground mine discharge from the Pittsburgh coal seam located in Lowber, PA (Westmoreland County), where a coal processing and coking facility were housed at one time. The mine was closed in the 1930s and a discharge developed in the 1940s. Water flowed from the entry down a 360-meter-long shallow channel to the receiving river. Over the next 60 years, the channel filled with 0.91 – 1.22 meters of sludge and vegetative debris. Chemical and flow characteristics of the discharge were determined in the 1970s by PA's Operation Scarlift program and recently by the authors. Flow rates range between 295,260 and 454,240 liters per hour, and do not appear to have changed substantially in 30 years. The chemistry of the discharge has changed over time, shifting from net acidic with approximately 200 mg/L Fe to net alkaline with 70-80 mg/L Fe. The discharge produces approximately 270,000 kg of dissolved iron per year, degrading two miles of the receiving creek.

3. Methods

Precipitate samples were collected in HDPE bottles at each location (Figure 13), both at the surface and at a depth of 0.6 meters. Samples were generally collected on the edges of the flow (flow was low as samples were collected in July). Sample 4S and 4S2 were collected on opposite sides of the flowing water, and it was not possible to collect samples at depth for these two locations. Sample 10C was collected at the point of discharge into the receiving creek. Samples collected at locations A and B are from an abandoned portion of the channel. In addition to precipitate samples, influent and effluent water samples were collected. If particulate matter was visible, the sample was filtered through a 0.45-micron cellulose acetate syringe filter prior to acidification to pH<2 with HCl. Field pH was measured using an Orion® 250A pH meter and field alkalinity was determined using the Hach® digital titration method.

Prior to analysis, splits of the precipitate samples were dried at <40˚C to prevent volatilization and potential loss of structural water, and visible organic matter was removed. Trace and major element concentrations in the water samples were determined using an inductively coupled plasma-atomic emission spectrometer (ICP-AES) at the U.S. Department of Energy National Energy Technology Laboratory (U.S. DOE NETL). Sulfate concentrations were determined by measuring total sulfur using ICP-AES. Total metals in the precipitate samples were analyzed by instrumental neutron activation analysis (INAA) and total acid digestion followed by ICP-AES analysis at Activation Laboratories in Ontario, Canada. Diffraction patterns were obtained using a Phillips X'pert powder diffractometer (Cu Kα radiation) at the Materials Science Laboratory, University of Pittsburgh. Back-filled powder mounted samples were scanned from 5 to 15˚ 2θ (0.5˚ divergence slit) and from 15 - 75˚ 2θ (1.0˚ divergence slit), and resulting peak positions were identified with the Phillips X'pert Organizer software. Morphological analysis was

conducted using a Phillips XL30 FEG scanning electron microscope (SEM) equipped with EDAX, also at the Materials Science Laboratory. Color measurements were made using a Datacolor International Spectraflash® 600 Plus spectrophotometer at the Graphic Arts Technical Foundation. Three additional samples were characterized as described above, including two natural iron oxides (Raw Sienna and Burnt Umber) obtained from a pigment company in the United States, as well as a grab sample collected at a later date form the Lowber channel. The Lowber sample was calcined (heated to 900°C) and milled (please see last section on resource recovery) prior to analysis.

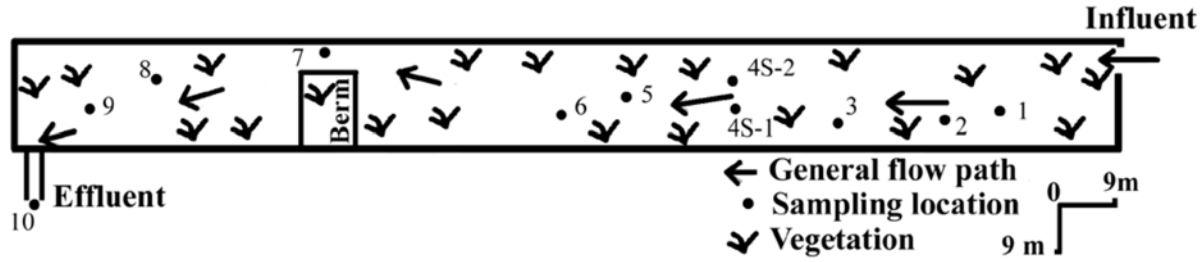

Figure 13. Schematic of Lowber channel and location of sampling points.

4. Results

4.1. Chemical Composition

Water quality remains constant from the influent end to the effluent end of the channel, with only a slight increase in pH (from 6.23 to 6.46; Table 8). The composition of the precipitates (Table 9) remains uniform both spatially and temporally, with some fluctuations in trace element composition (specifically Zn and Mn). The presence of As, Co, Ni and Zn in the precipitates at concentrations up to 100 mg/kg as compared to the water where most of the elements are below ppb levels, indicates that the precipitates are sorbing trace elements out of proportion to their concentration in the water, which is consistent with past findings (Chapman et al., 1983; Blowes and Jambor, 1990; Kairies et al., 2002). Calcining results in conversion of some of the goethite to hematite. Iron concentrations in the natural iron oxide samples analyzed are 20 – 30% less than that in the Lowber precipitate samples. Additionally, concentrations of Mn, Ni and Zn in these two samples are two to three orders of magnitude higher than the other samples.

4.2. Mineralogy and Morphology

All the Lowber samples are comprised of goethite with minor amounts of quartz (resulting from influx of sediment during flooding and normal rainfall runoff events). The precipitates remain crystalline both at the surface and at depth (L-5S and L-5D, (e.g., Figure 14)), as well as throughout the channel. The natural iron oxide samples contain lepidocrocite in addition to goethite and quartz. The calcined Lowber sample contains both hematite and goethite (Figure 15), as well as some quartz.

The Lowber samples exhibit spherical morphologies: globular (Figure 16) and hedgehog-like/spiky (Figure 17), both of which occur as aggregated particles. The calcined Lowber sample

also contain aggregated spherical (globular, Figure 18) particles, though the surfaces appear smoother than the other Lowber samples. The natural iron oxide samples contain platy, spherical (globular) and acicular particles (Figure 19), all of which do not appear to be aggregated.

Table 8. Lowber water chemistry (mg/L).

	pH	Alkalinity[a]	Fe	Al	Ca	Mg	Na	SO_4^{2-}	Cr	Mn
Influent	6.23	330	77	0	170	44	489	1182	0.01	1.4
Effluent	6.46	320	72	0	176	45	473	1192	0.01	1.4

[a]As $CaCO_3$

As<0.08; Co, Zn<0.006; Ni<0.010

Table 9. Lowber precipitate and natural iron oxide chemistry* in wt.% (where noted) or mg/kg.

Sample	Fe %	Al %	Mg %	Na %	S %	As	Cd	Co	Cr	Mn	Ni	Zn
L-1S	50	0.37	0.01	0.08	0.15	43.1	3	3	10	123	7.1	8.8
L-1D	41	0.81	0.05	0.17	0.15	14.6	2	7	41	369	9.1	24.3
L-2S	51	0.36	0.10	0.20	0.25	11.0	2	6	16	348	6.6	19.1
L-2D	54	0.30	0.02	0.12	0.18	23.4	4	6	6	217	5.6	14.3
L-3S	54	0.15	<0.01	0.08	0.16	41.3	2	3	7	144	3.2	5.8
L-3D	56	0.11	<0.01	0.10	0.17	21.8	4	6	<0.3	241	3.7	5.4
L-4S	54	0.08	<0.01	0.07	0.17	36.8	3	3	<0.3	165	2.2	4.7
L-4S2	52	0.25	0.05	0.14	0.18	16.0	2	5	7	675	7.8	10.7
L-5S	54	0.08	<0.01	0.10	0.18	27.0	3	7	<0.3	320	3.7	5.8
L-5D	56	0.08	<0.01	0.12	0.16	17.1	4	5	8	249	4.6	5.5
L-6S	53	0.34	<0.01	0.02	0.10	10.2	3	8	13	293	9.4	15.3
L-6D	45	0.81	0.05	0.12	0.13	28.0	2	6	28	247	15.3	41.2
L-7S	58	0.10	<0.01	0.06	0.16	15.6	2	4	9	238	2.2	6.5
L-7D	58	0.16	<0.01	0.11	0.17	20.8	3	3	11	189	2.7	73.0
L-8S	57	0.11	<0.01	0.03	0.14	15.8	4	5	<0.3	309	5.1	7.6
L-8D	57	0.26	0.01	0.08	0.16	19.4	3	5	10	191	7.8	53.0
L-9S	57	0.13	0.01	0.10	0.18	24.8	3	4	<0.3	304	4.3	59.0
L-9D	55	0.12	0.03	0.08	0.15	23.8	2	4	<0.3	264	3.6	9.1
L-10C	54	0.03	<0.01	0.10	0.27	23.4	3	3	<0.3	232	2.6	<0.1
L-AS	57	0.10	<0.01	<0.01	0.11	11.3	3	4	8	247	7.2	121.0
L-AD	53	0.36	0.02	0.03	0.13	11.8	2	4	16	193	8.5	109.0
L-BS	55	0.19	<0.01	0.01	0.09	20.2	2	5	13	275	8.4	12.9
L-BD	51	0.46	0.03	0.05	0.10	17.9	3	6	12	209	7.1	18.9
st. dev.	4	0.21	0.03	0.05	0.04	9.1	1	1	9	109	3.1	33.9
L-calcine	50	1.25	0.05	0.07	0.293	57	<0.3	12	10	786	40	389
Burnt Umber	26	4.12	0.26	0.04	0.05	43	10	42	62	16176	110	2400
Raw Sienna	30	3.30	0.31	0.03	0.02	41	22	124	42	6136	240	3850

[a]Ca < DL of 0.01%, except: L1S, L1D=0.03%; L2S=0.18%; L4S=0.05%; L4S2, L5S=0.08%; L9S=0.06%; L10C=0.46%

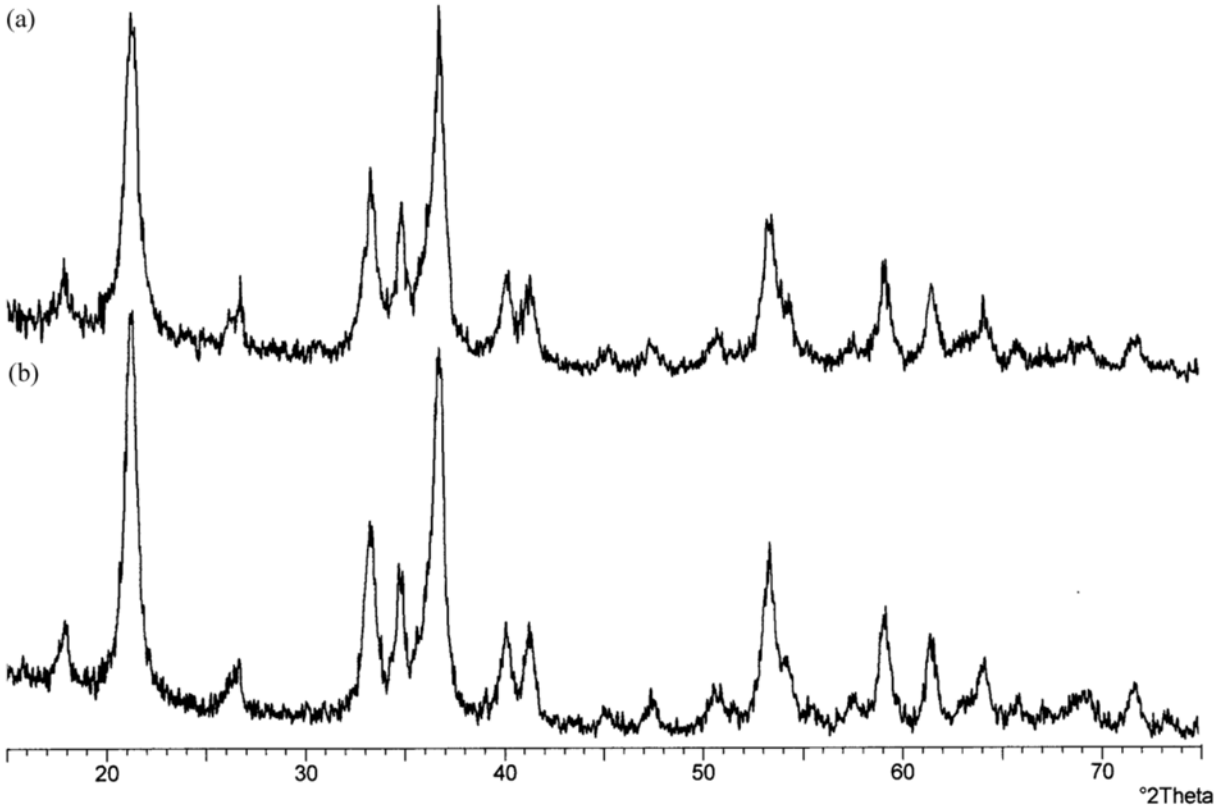

Figure 14. Representative XRD pattern of Lowber precipitates (a) surface; (b) deep.

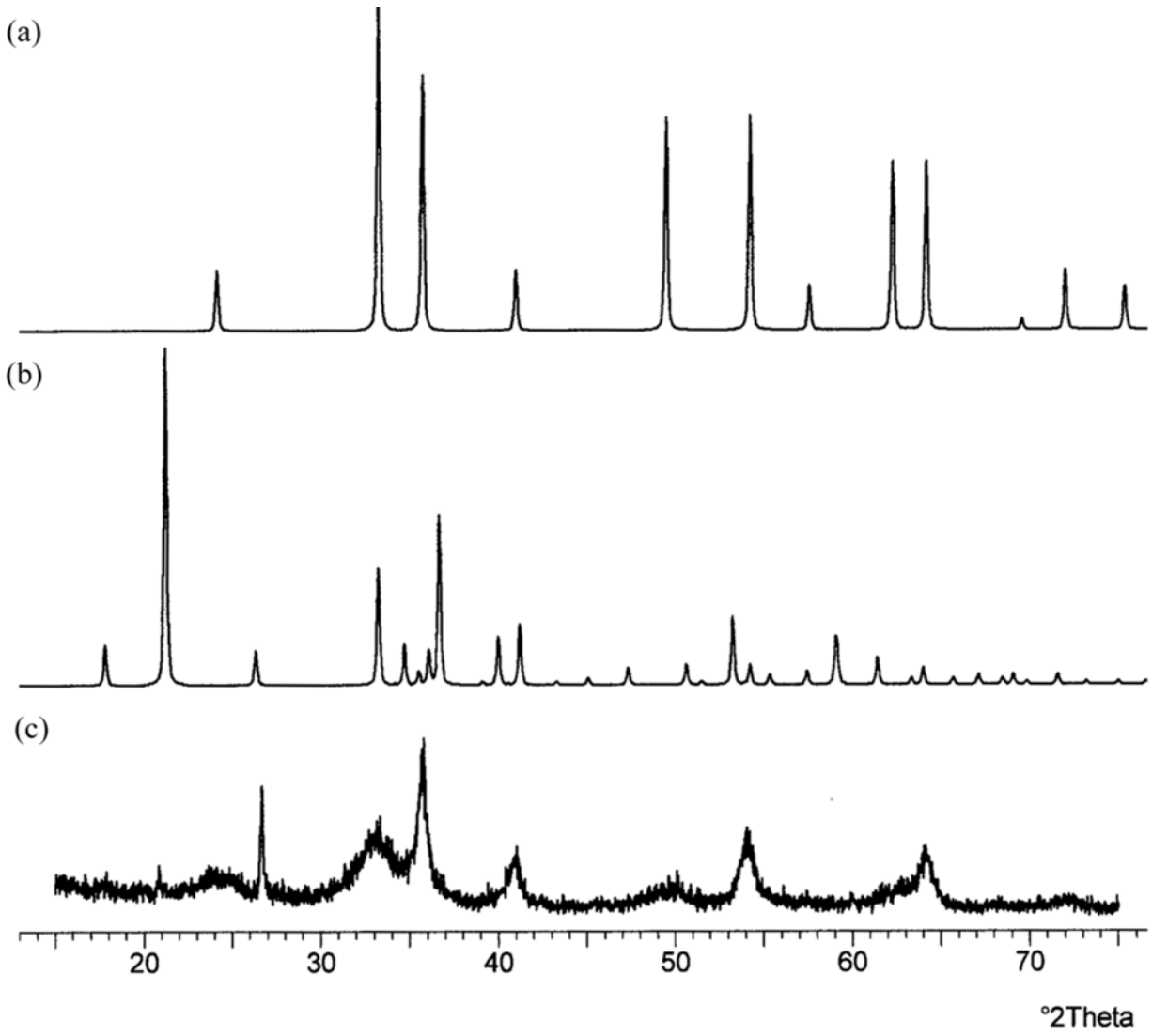

Figure 15. Diffraction patterns for (a) ideal hematite; (b) ideal goethite; (c) Lowber (calcined).

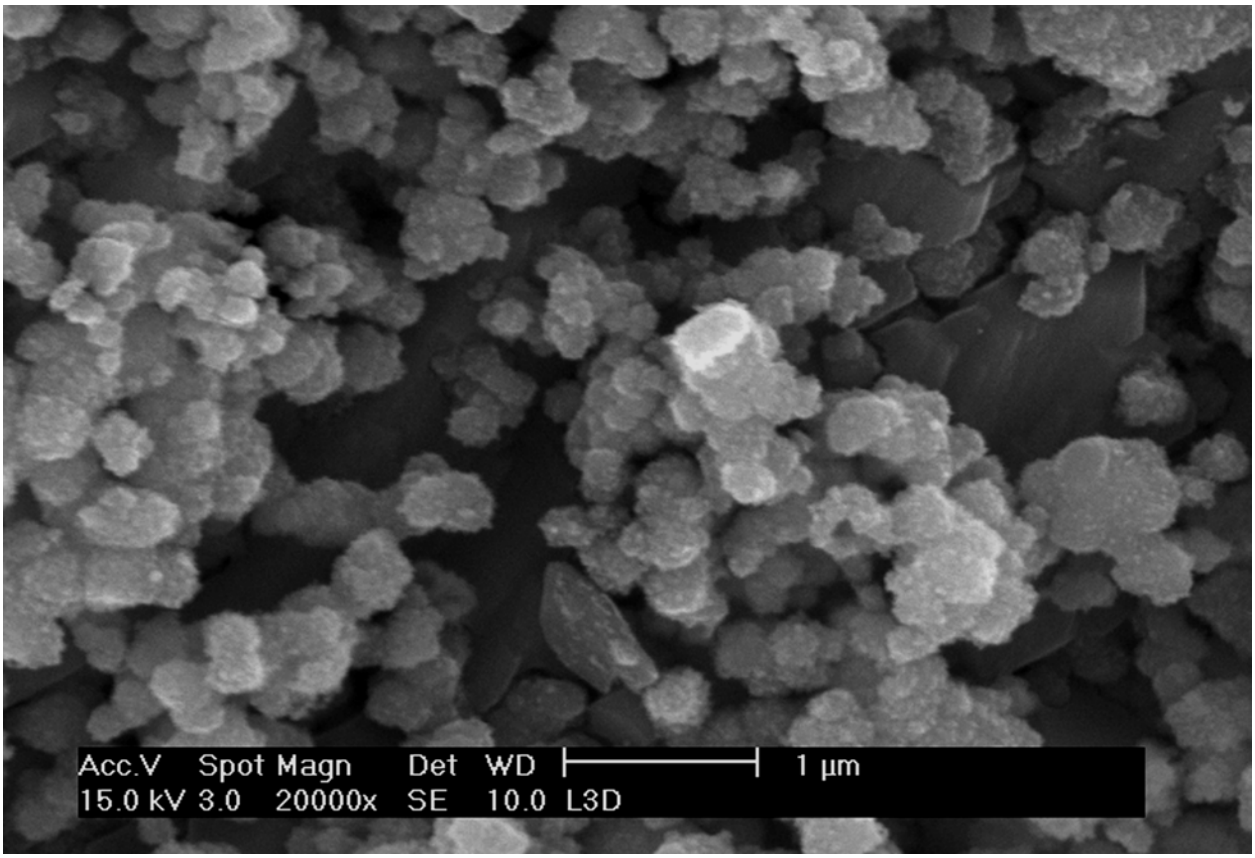

Figure 16. Globular morphology seen in precipitates collected from Lowber.

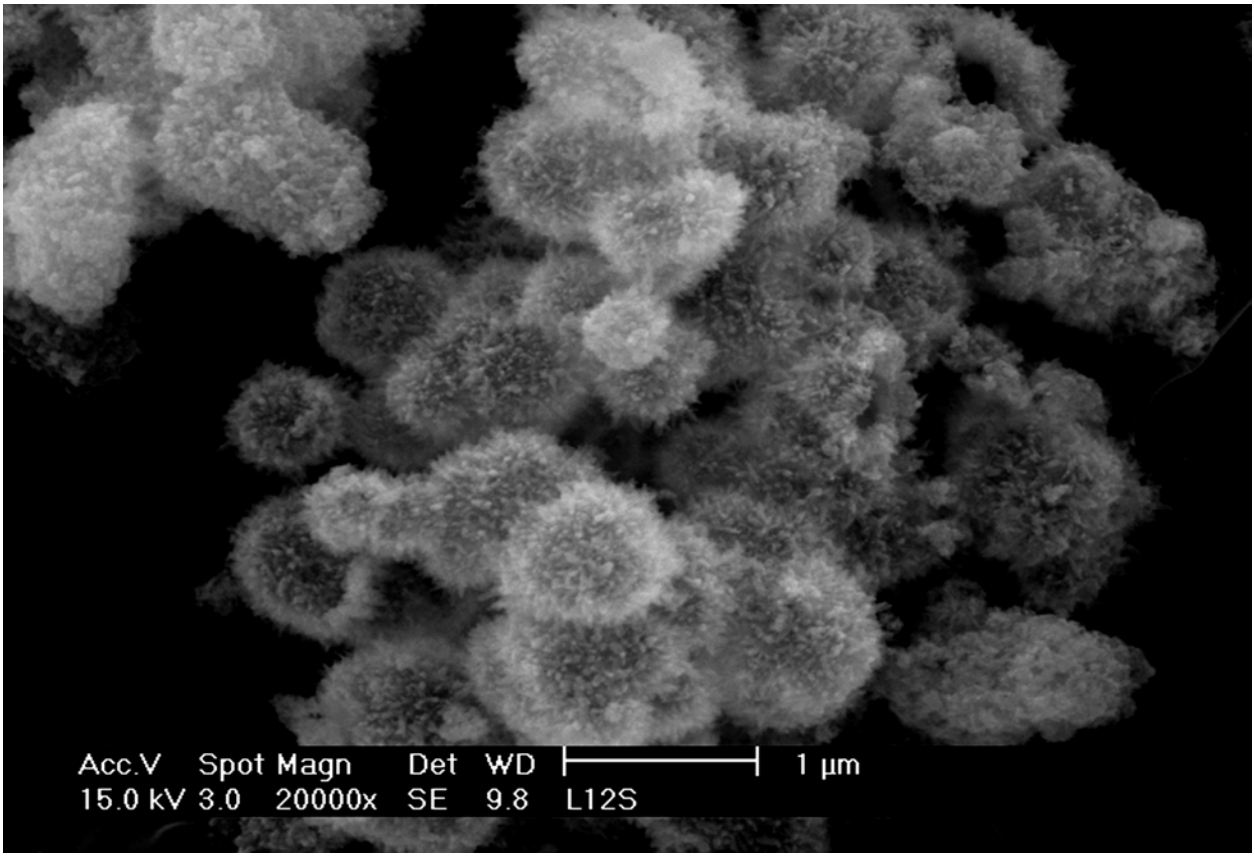

Figure 17. Spiky morphology seen in precipitates collected from Lowber.

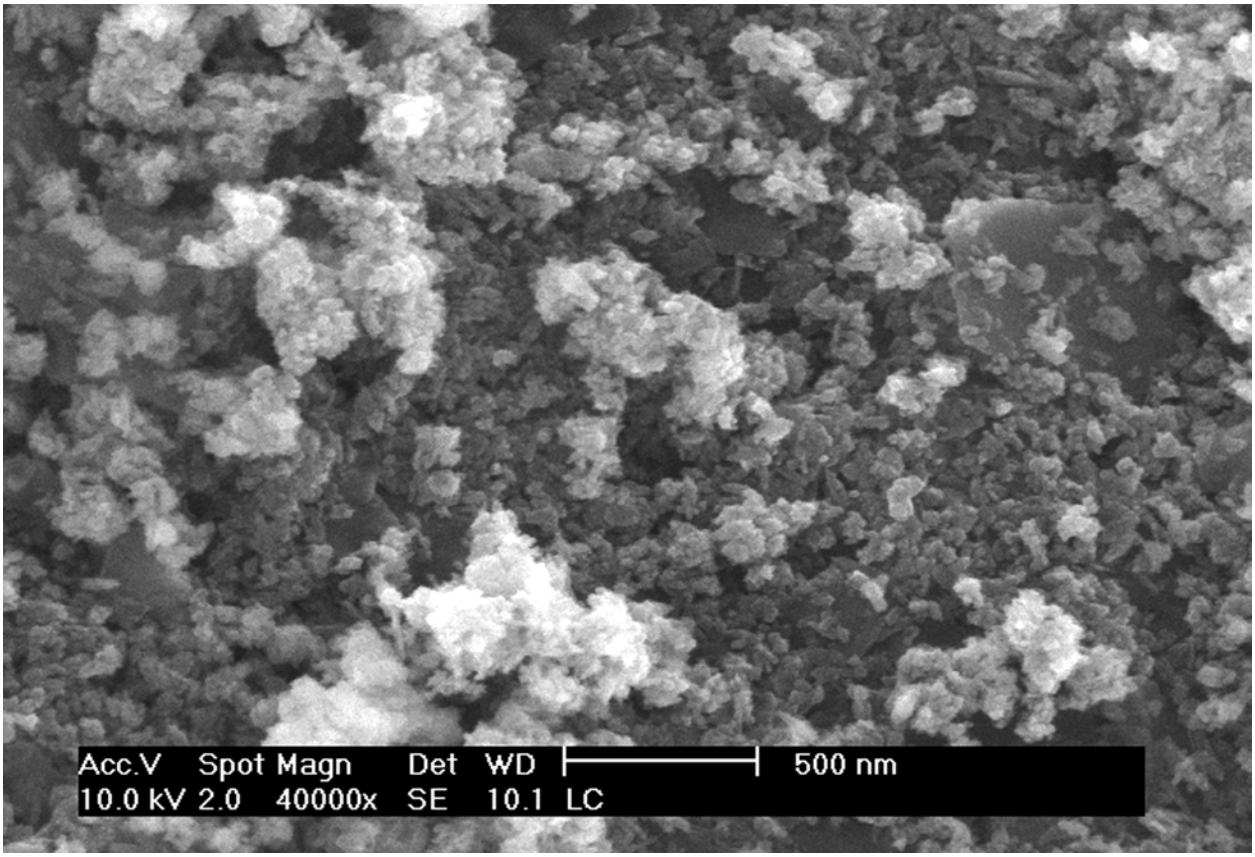

Figure 18. Calcined Lowber sample.

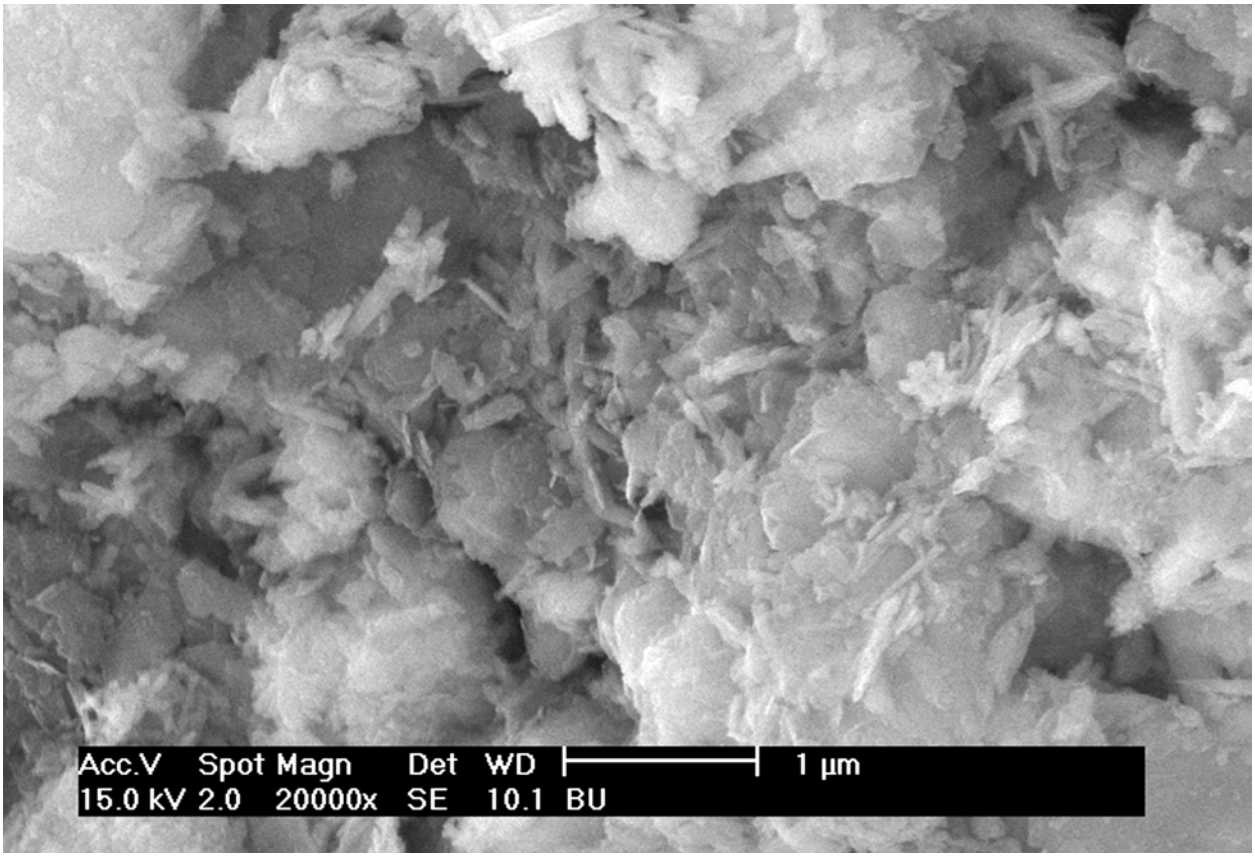

Figure 19. Natural iron oxide sample.

4.3. Color

Color data (Table 10) are in the CIELAB notation, which defines each sample's color as a position in three-dimensional color space (Figure 20). L* defines lightness, a* defines the red/green component and b* defines the yellow/blue component. Color differences (ΔL*, Δa*, and Δb*) can be determined between a sample and a reference standard, where the L*, a* and b* values for the reference standard are subtracted from those of the sample. Total color difference (ΔE*) between two samples can be calculated in the following manner:

$$\Delta E^* = [(\Delta L^*)^2 + (\Delta a^*)^2 + (\Delta b^*)^2]^{1/2}$$

Total color differences (Table 10) were determined between the sample collected at the surface and the sample collected at depth (defined by the authors as the reference standard) for a given sampling point. Color difference for samples 4S and 4S2 were also calculated. The Lowber samples exhibit little spatial or temporal color variability (Figure 21). The calcined Lowber sample has the highest a* value (28.87) compared to the other samples, indicating the other samples are not as red. The calcined Lowber and the Burnt Umber have the lowest b* values (30.63 and 25.46, respectively), indicating they have the lowest yellow component (approaching green), while the Raw Sienna has the highest b* value (39.18).

A redness index (RI) was calculated in the following manner (based on Barron and Torrent, 1986):

$$RI = [a^*(a^{*2} + b^{*2})^{1/2}(10^{10})]/b^*L^{*6}$$

The values are listed in Table 10.

Table 10. Color measurement values.

Location	L*	a*	b*	dE*	RI
L-1S	60.04	16.89	33.40	3.24	4.04
L-1D	61.26	14.96	35.70		3.07
L-2S	59.35	16.43	33.91	4.37	4.18
L-2D	61.91	16.60	37.45		3.22
L-3S	60.13	16.65	33.53	3.38	3.93
L-3D	61.28	16.61	36.71		3.44
L-4S	59.61	16.10	32.40	3.01	4.01
L-4S2	60.02	17.60	34.98		4.21
L-5S	62.64	16.48	35.95	2.30	3.00
L-5D	60.40	16.39	35.45		3.72
L-6S	59.25	17.94	34.63	1.99	4.67
L-6D	60.73	16.80	35.31		3.71
L-7S	61.99	16.23	37.05	0.99	3.12
L-7D	61.01	16.37	37.04		3.47
L-8S	62.11	17.11	38.12	2.82	3.27
L-8D	59.97	17.40	36.30		4.15
L-9S	59.85	16.15	33.61	3.78	3.90
L-9D	62.46	16.03	36.34		2.95
L-10C	63.00	15.72	33.13		2.78
L-AS	59.67	18.48	34.86	2.13	4.63
L-AD	58.15	17.74	33.56		5.19
L-BS	60.35	17.85	35.73	1.63	4.13
L-BD	59.09	17.91	34.70		4.73
st. dev.	1.28	0.84	1.54		0.65
L-calcine	34.69	28.87	30.63		227.65
Burnt Umber	44.24	10.44	25.46		15.05
Raw Sienna	55	12.9	39.18		4.91

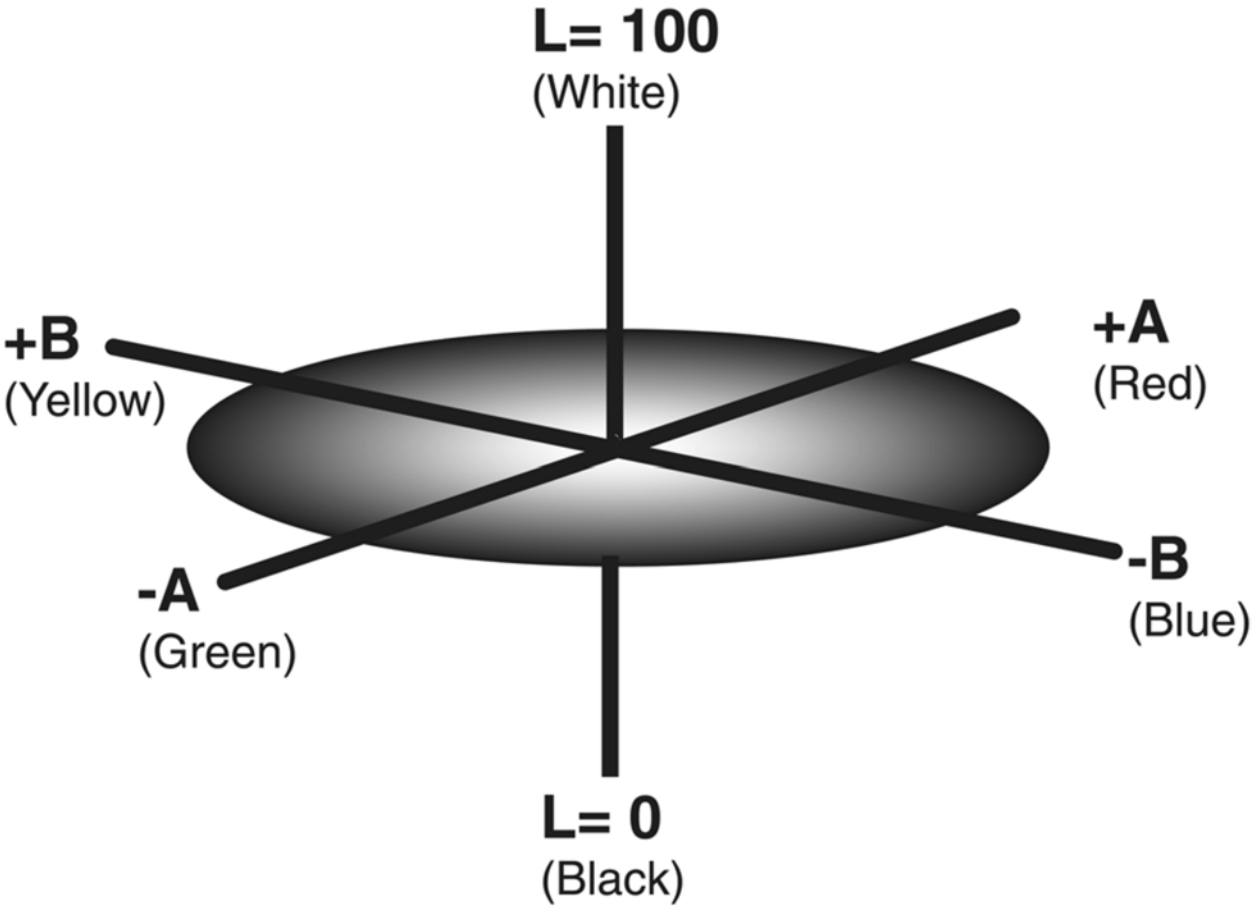

Figure 20. Schematic of CIELAB color space.

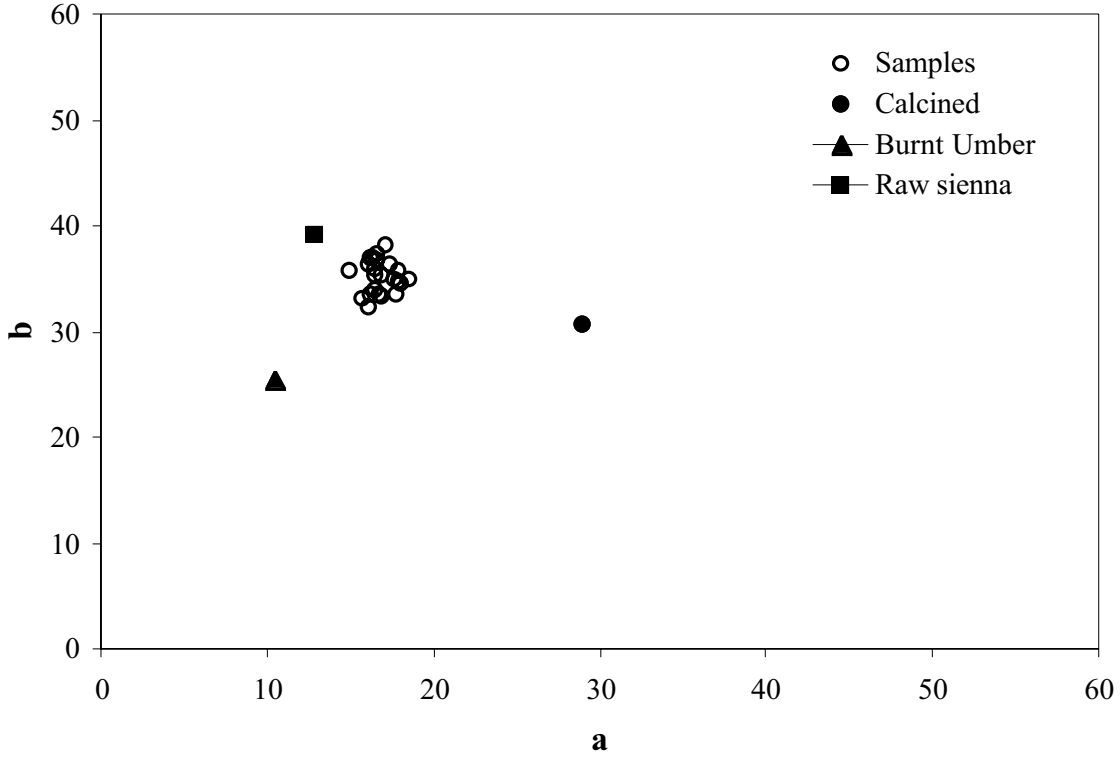

Figure 21. Position of samples in CIELAB color space.

5. Discussion and Conclusion

5.1. Precipitate Homogeneity

The precipitates formed in the Lowber channel are all moderately crystalline goethite with slight variations in morphology and elemental composition. Principle component analysis showed that the variance in elemental composition was due primarily to the concentrations of Fe, Al, and As. No correlation exists between elemental concentrations and the color parameters (all r^2 values are < 0.1) or the redness index (all r^2 values are < 1.0). Principle component analysis indicates that the variance in color arises from the L* (lightness) component rather than changes in hue. No significant differences were found between the samples collected at the surface and those collected at depth. Although the calcined Lowber sample is red (not yellow brown as the other Lowber samples), it has not undergone complete transformation from goethite to hematite as indicated by results from XRD and SEM analyses.

The relationship between color and elemental concentration of the samples is tenuous at best. It is evident that factors other than elemental composition impact the resulting color of the sample. Mineral structure, degree of crystallinity, compaction, packing, aggregation and particle size distribution are all factors that potentially contribute to the resulting color.

5.2. Comparison of Mine Drainage Precipitates to Natural Iron Oxides

Based on the fact that the mine drainage precipitates contain 20 – 30 % more Fe and that Mn, Ni and Zn concentrations are up to three orders of magnitude lower than in the natural iron oxides, the mine drainage precipitates are of a higher purity. The presence of trace elements can influence the resulting color of the sample, particularly Mn (which will cause a greenish brown

color) (Mauney, 1994; Cornell and Schwertmann, 1996). The Burnt Umber sample is greener than any of the other samples due to the high Mn concentrations (1.6 dry wt. %) as compared to the other samples.

Results of this study indicate that mine drainage precipitates formed at the Lowber site (and potentially other net-alkaline mine discharges) are suitable for use as a pigment, due to their relatively uniform color and purity. The results also show that the creation of a predictive geochemical model for the formation of coal mine drainage precipitates is complex and cannot be based solely on the chemistry of the discharge. Precipitates examined in this study show promise for resource recovery, though each site must be considered on a case by case basis.

It may be possible to use the precipitates for purposes other than as a pigment. Iron oxides and hydroxides are known to preferentially sorb metals out of solution and incorporate them into the iron oxide/hydroxide structure. Sorption processes are influenced by the degree of crystallinity, pH of the water, and dissolved constituents, among other things. As a result of these associations, the precipitates can be effective sinks and concentrators for trace metals (e.g., aluminum, arsenic, copper, manganese, nickel and zinc). Because of this, it may be possible to utilize coal mine drainage precipitates in the clean-up of contaminated groundwater (similar to a permeable reactive barrier) or polluted surface water. Further research is necessary to evaluate this potential.

Whether it is economical to pursue extraction of these metals from the precipitates depends on the concentration and the current market value of the individual metal, and is beyond the scope of this paper. It is often difficult to extract only one metal of interest during an extraction procedure, and the extracting solution can cost more than the value of the recovered metal. Alternatively, the precipitates could be dredged and hauled to a landfill adding to the operation

and maintenance costs of the treatment system. Precipitate dewatering prior to transport is necessary and represents another ongoing cost.

5.3. Resource Recovery Effort

Lowber became the focus of a resource recovery project headed by Robert S. Hedin (Hedin Environmental, Pittsburgh, PA), who was contracted to supply 1000 tons of filtercake with about 45% solids (in-place iron oxide sludge is about 25% solids) to a pigment company in an effort to produce about 270,000 kg of dry processed iron oxide product.

The processing of the Lowber product to a finished pigment involved drying, classification, calcination, milling, and blending. Classification removed large debris. During calcination the product was heated to ~900^{o}C, which dehydrated the goethite to hematite (Fe_2O_3) and volatilized any remaining organic contaminants (vegetation and coal). Milling decreased the product particle size to the 0.5-5 micron range. The final product was blended with other materials to yield finished pigments. The finished Lowber project was superior in several pigmentary characteristics to finished products produced from natural goethite ores. However, the Lowber material was difficult to handle and dry because its moisture content (50%) was substantially higher than mined iron oxide products (<10% moisture).

At this time, the value of the mine drainage product is limited by the price of competitive mined products – $100-400 per ton (Potter, 2000). These product values are not sufficient to support the construction of mine drainage treatment systems. Systems designed to treat mine water and produce a marketable iron product are currently projected to cost approximately $500 per ton of iron oxide recovered. The product values do appear to be sufficient to support the management and long-term operation and maintenance of treatment systems. If the system is

constructed in a manner to facilitate sludge recovery, iron oxides can be produced for $200-300 per ton (dry weight).

BIBLIOGRAPHY

Ali, M.A. and Dzombak, D.A., 1996a. Effects of simple organic acids on sorption of Cu^{2+} and Ca^{2+} on goethite. Geochim. Cosmochim. Acta 60(2), 291-304.

Ali, M.A. and Dzombak, D.A., 1996b. Interactions of copper, organic acids, and sulfate in goethite suspensions. Geochim. Cosmochim. Acta 60(24), 5045-5053.

Balistrieri, L.S. and Murray, J.W., 1982. The adsorption of Cu, Pb, Zn, and Cd on goethite from major ion seawater. Geochim. Cosmochim. Acta 46, 1253-1265.

Barron, V. and Torrent, J., 1986. Use of the Kubelka-Munk theory to study the influence of iron oxides on soil colour. J. Soil Sci. 37, 499-510.

Beckett, P.H.T., 1989. The use of extractants in studies on trace metals in soils, sewage sludges, and sludge-treated soils. Adv. Soil Sci. 9, 144-176.

Benjamin, M.M. and Leckie, J.O., 1980. Multiple site adsorption of Cd, Cu, Zn, and Pb on an amorphous iron oxyhydroxide. J. Colloid Interface Sci. 79(209).

Bigham, J.M., Schwertmann, U. and Carlson, L., 1992. Mineralogy of precipitates formed by the biogeochemical oxidation of Fe(II) in mine drainage. Catena Suppl. 21, 219-232.

Blowes, D.W. and Jambor, J.L., 1990. The pore water geochemistry and the mineralogy of the vadose zone of sulfide tailings. Appl. Geochem. 5, 327-346.

Butler, J.N., 1964. Ionic Equilibrium. Addison-Wesley Publishing Company, Reading, MA, 559 p.

Brady, K.B.C., Hornberger, R.J., and Fleeger, G., 1998. Influence of geology on postmining water quality: Northern Appalachian Basin. In: K.B.C. Brady, M.W. Smith, and J. Schueck (Editors), Coal Mine Drainage Prediction and Pollution Prevention in Pennsylvania, pp. 8-1 – 8-83.

Burns, R.G. and Burns, V.M., 1977. Mineralogy of ferromanganese nodules. In: G.P. Glasby (Editor), Marine Manganese Deposits. Elsevier, pp. 185-248.

Capo, R.C., Winters, W.R., Weaver, T.J., Stafford, S.L., Hedin, R.S. and Stewart, B.W., 2001. Hydrogeologic and geochemical evolution of deep coal mine discharges, Irwin syncline, Pennsylvania, 22nd Annual West Virginia Surface Mine Drainage Symposium, pp. 144-153.

Carlson, L. and Schwertmann, U., 1981. Natural ferrihydrites in surface deposits from Finland and their association with silica. Geochim. Cosmochim. Acta 45, 421-429.

Chapman, B.M., Jones, D.R. and Jung, R.F., 1983. Processes controlling metal ion attenuation in acid mine drainage streams. Geochim. Cosmochim. Acta 47, 1957-1973.

Childs, C.W., Inoue, K. and Mizota, C., 1998. Natural and anthropogenic schwertmannites from Towada-Hachimantai National Park, Honshu, Japan. Chem. Geol. 144, 81-86.

Code of Federal Regulations, 2000. Title 21.

Collins, C.R., Ragnarsdottir, K.V. and Sherman, D.M., 1999. Effect of inorganic ligands on the mechanism of cadmium sorption to goethite. Geochim. Cosmochim. Acta 63(19/20), 2989-3002.

Cornell, R.M. and Schwertmann, U., 1996. The Iron Oxides: Structure, Properties, Reactions, Occurrences and Uses. VCH, Weinheim, 573 p.

Coughlin, B.R. and Stone, A.T., 1995. Nonreversible adsorption of divalent metal ions (Mn, Co, Ni, Cu, and Pb) onto goethite: effects of acidification, Fe(II) addition, and picolinic acid addition. Environ. Sci. Technol. 29, 2445-2455.

Davidson, C.M., Duncan, A.L., Littlejohn, D., Ure, A.M. and Garden, L., 1998. A critical evaluation of the three-stage BCR sequential extraction procedure to assess the potential mobility and toxicity of heavy metals in industrially-contaminated land. Anal. Chim. Acta 363, 44-55.

Domingo, C., Rodríguez-Clemente, R. and Blesa, M., 1994. Morphological properties of _-FeOOH, _-FeOOH and Fe_3O_4 obtained by oxidation of aqueous Fe(II) solutions. J. Colloid Interface Sci. 165, 244-252.

Dzombak, D.A. and Morel, F.M.M., 1990. Surface Complexation Modeling: Hydrous Ferric Oxide. John Wiley & Sons, New York, 393 p.

Esmadi, F. and Simm, J., 1995. Sorption of cobalt (II) by amorphous ferric hydroxide. Coll. Sur. 104, 265-270.

Fales, H.A. and Kenny, F., 1940. Inorganic Quantitative Analysis. D. Appleton Century Co., New York, 713 p.

Fish, C.L., Hedin, R.S. and Partezana, J.M., 1996. Chemical characterization of iron oxide precipitates from wetlands constructed to treat polluted coal mine drainage, National Meeting of the American Society for Surface Mining and Reclamation, Knoxville, TN, pp. 541-549.

Gerth, J., 1990. Unit-cell dimensions of pure and trace metal-associated goethites. Geochim. Cosmochim. Acta 54, 363-371.

Giovanoli, R. and Cornell, R.M., 1992. Crystallization of metal substituted ferrihydrites. Z. Pflanzenernähr. Bodenk. 155, 455-460.

Gómez-Ariza, J.L., Giráldez, I., Sánchez-Rodas, D. and Morales, E., 1999. Metal readsorption and redistribution during the analytical fractionation of trace elements in oxic estuarine sediments. Anal. Chim. Acta 339, 295-307.

Gómez-Ariza, J.L., Giráldez, I., Sánchez-Rodas, D. and Morales, E., 2000. Comparison of the feasibility of three extraction procedures for trace metal partitioning in sediments from south-west Spain. Sci. Tot. Environ. 246, 271-283.

Hedin, R.S., 1996. Recovery of iron oxides from polluted coal mine drainage. Technical proposal for a patent application filed with the U.S. Patent and Trademark Office, pp. 1-32.

Hedin, R.S., 1998. Potential recovery of iron oxides from coal mine drainage, Nineteenth Annual West Virginia Surface Mine Drainage Task Force Symposium, West Virginia University, Morgantown, WV.

Hedin, R.S., Nairn, R.W. and Kleinmann, R.L.P., 1994. Passive Treatment of Coal Mine Drainage. Information Circular 9389, U.S. Bureau of Mines, Washington, D.C, 35 p.

Hem, J.D., 1964. Deposition and solution of manganese oxides. Water-Supply Paper 1667-B, U. S. Geol. Surv.

Hem, J.D., 1977. Reactions of metal ions at surfaces of hydrous iron oxide. Geochim. Cosmochim. Acta 41, 527-538.

Hem, J.D., 1992. Study and Interpretation of the Chemical Characteristics of Natural Water, Third edition. USGS Water Supply Paper 2254, 263 p.

Herbert, R.B., Jr., 1996. Metal retention by iron oxide precipitation from acidic ground water in Dalarna, Sweden. Appl. Geochem. 11, 229-235.

Honeyman, B.D. and Leckie, J.O., 1986. Macroscopic partitioning coefficients for metal ion adsorption, American Chemical Society Symposium Series, pp. 162-190.

Hudson-Edwards, K.A., Schell, C. and Macklin, M.G., 1999. Mineralogy and geochemistry of alluvium contaminated by metal mining in the Rio Tinto area, southwest Spain. Appl. Geochem. 14, 1015-1030.

Jenne, E.A., 1968. Controls on Mn, Fe, Co, Ni, Cu, and Zn concentrations in soils and water: the significant role of hydrous Mn and Fe oxides, Trace Inorganics in Water. Advances in Chemistry Series, Number 73. American Chemical Society, pp. 327-387.

Jeon, B.-H., 1998. The characterization of iron oxides produced from passive treatment of mine drainage, MS Thesis, The Pennsylvania State University, 156 p.

Kairies, C.L., Capo, R.C., Hedin, R.S. and Watzlaf, G.R., 2000. Characterization of iron-rich mine drainage precipitates associated with Allegheny and Monongahela group coals. *Geol. Soc. Amer.* Abstracts with Programs 32, A-477.

Kairies, C.L., Capo, R.C. and Watzlaf, G.R., 2002. Development and evaluation of sequential extraction procedures for iron-rich precipitates associated with coal mine drainage. In: Proceedings of the National Meeting of the American Society for Mining and Reclamation, Lexington, KY, p. 1192.

Karathanasis, A.D. and Thompson, Y.L., 1995. Mineralogy of iron precipitates in a constructed acid mine drainage wetland. Soil Sci. Soc. Am. J. 59, 1773-1781.

Karlsson, S., Allard, B. and Håkansson, K., 1988. Chemical characterization of stream-bed sediments receiving high loadings of acid mine effluents. Chem. Geol. 67, 1-15.

Karthikeyan, K.G., Elliott, H.A. and Cannon, F.S., 1997. Adsorption and coprecipitation of copper with the hydrous oxides of iron and aluminum. Environ. Sci. Technol. 31, 2721-2725.

Keon, N.E., Swartz, C.H., Brabander, D.J., Harvey, C. and Hemond, H.F., 2001. Validation of an arsenic sequential extraction method for evaluating mobility in sediments. Envron. Sci. Technol 35, 2778-2784.

Kheboian, C. and Bauer, C.F., 1987. Accuracy of selective extraction procedures for metal speciation in model aquatic sediments. Anal. Chem. 59, 1417-1423.

Kirby, C.S., Decker, S.M. and Macander, N.K., 1999. Comparison of color, chemical and mineralogical compositions of mine drainage sediments to pigment. Environ. Geol. 37(3), 243-254.

Kühnel, R.A., Roorda, H.J. and Steensma, J.J., 1975. The crystallinity of minerals: A new variable in pedogenetic processes: A study of goethite and associated silicates in laterites. Clays and Clay Min. 23, 349-354.

Lindsay, W.L. and Norvell, W.A., 1978. Development of a DTPA soil test for zinc, iron, manganese and copper. Soil Sci. Soc. Am. J. 42, 421-428.

Lovley, D.R. and Phillips, E.J.P., 1987. Rapid assay for microbially reducible ferric iron in aquatic sediments. Appl. Environ. Microbiol. 53, 1536-1540.

Maiz, I., Esnaola, V. and Millán, E., 1997. Evaluation of heavy metal availability in contaminated soils by a short sequential extraction procedure. Sci. Tot. Environ. 206, 107-115.

Manceau, A., Schlegel, M.L., Musso, M., Sole, V.A., Gauthier, C., Petit, P.E. and Trolard, F., 2000. Crystal chemistry of trace elements in natural and synthetic goethite. Geochim. Cosmochim. Acta 64(21), 3643-3661.

Martin, R., Sanchez, D.M. and Gutierrez, A.M., 1998. Sequential extraction of U, Th, Ce, La, and some heavy metals in sediments from Ortigas river, Spain. Talanta 46, 1115-1121.

Martínez, C.E. and McBride, M.B., 1998. Solubility of Cd^{2+}, Cu^{2+}, Pb^{2+}, and Zn^{2+} in aged coprecipitates with amorphous iron hydroxides. Environ. Sci. Technol. 32, 743-748.

Mauney, S.S., 1994. Natural iron oxides pigments - rebirth through innovation. Mining Eng., 70-73.

McCarty, D.K., Moore, J.N. and Marcus, A.W., 1998. Mineralogy and trace elemental association in an acid mine drainage iron oxide precipitate: comparison of selective extractions. Appl. Geochem. 13, 165-176.

Mester, Z., Cremisini, C., Ghiara, E. and Morabito, R., 1998. Comparison of two sequential extraction procedures for metal fractionation in sediment samples. Anal. Chim. Acta 359, 133-142.

Munk, L.A., Faure, G., Pride, D.E. and Bigham, J.M., 2002. Sorption of trace metals to an aluminum precipitate in a stream receiving acid rock-drainage; Snake River, Summit County, Colorado. Appl. Geochem. 17, 421-430.

Nirel, P.M. and Morel, F.M.M., 1990. Pitfalls of sequential extraction. Wat. Res. 24(8), 1055-1056.

Pennsylvania Department of Environmental Protection, 1998. *Healing the land and water: Pennsylvania's Abandoned Mine Reclamation Program.* 5000-BK-DEP2274, Department of Environmental Protection.

Pierce, M.L. and Moore, C.B., 1980. Adsorption of arsenite on amorphous iron hydroxide from dilute aqueous solution. Environ. Sci. Technol. 14(2), 214-216.

Potter, M.J., 2000. Iron Oxide Pigments, 2000 Annual Review, U. S. Geological Survey Minerals Yearbook: 1999. U. S. Dept. of the Interior, Washington, D. C.

Quevauviller, P., Rauret, G., López-Sánchez, J.-F., Rubio, R., Ure, A.M. and Muntau, H., 1997. Certification of trace metal extractable contents in a sediment reference material (CRM 601) following a three-step sequential extraction procedure. Sci. Tot. Environ. 205, 223-234.

Raksasataya, M., Langdon, A.G. and Kim, N.D., 1996. Assessment of the extent of lead redistribution during sequential extraction by two different methods. Anal. Chim. Acta 332, 1-14.

Rauret, G., Lopez-Sanchez, J.F., Rubio, R., Davidson, C.M., Ure, A.M. and Muntau, H., 1999. Improvement of the BCR three-step sequential extraction procedure prior to the certification of new sediment and soil reference materials. J. Environ. Monitor. 1, 57-61.

Roscoe, H.C., 1999. Evaluation of passive systems for the treatment of mine drainage. MS Thesis, The Pennsylvania State University, 213 p.

Rose, A.W. and Bianchi-Mosquera, G.C., 1993. Adsorption of Cu, Pb, Zn, Co, Ni, and Ag on goethite and hematite: a control on metal mobilization from red beds into stratiform copper deposits. Econ. Geol. 88, 1226-1236.

Saeki, K. and Matzumoto, S., 1994. Common. Soil Sci. and Plant Anal. 25, 2147.

Sahuquillo, A., López-Sánchez, J.F., Rubio, R., Rauret, G., Thomas, R.P., Davidson, C.M. and Ure, A.M., 1999. Use of a certified reference material for extractable trace metals to assess sources of uncertainty in the BCR three-stage sequential extraction procedure. Anal. Chim. Acta 382, 317-327.

Schindler, P.W., 1990. Co-adsorption of metal ions and organic ligands: formation of ternary surface complexes. In: M.F.J. Hochella and A.F. White (Editors), Mineral-water interface geochemistry. Reviews in Mineralogy. Mineralogical Society of America, Washington.

Schwertmann, U., Cambier, P. and Murad, E., 1985. Properties of goethites of varying crystallinity. Clays and Clay Min. 33(5), 369-378.

Schwertmann, U. and Cornell, R.M., 1991. *Iron Oxides in the Laboratory: Preparation and Characterization*. VCH, Weinheim, 204 p.

Stumm, W. and Morgan, J., 1970. Aquatic Chemistry. Wiley-Interscience, New York, 583 p.

Sutherland, R.A., 2002. Comparison between non-residual Al, Co, Cu, Fe, Mn, Ni, Pb and Zn released by a three-step sequential extraction procedure and a dilute hydrochloride acid leach for soil and road deposited sediment. Appl. Geochem. 17, 353-365.

Sutherland, R.A. and Tack, F.M.G., 2002. Determination of Al, Cu, Fe, Mn, Pb and Zn in certified reference materials using the optimized BCR sequential extraction procedure. Anal. Chim. Acta 454, 249-257.

Tarutis, W.J. and Unz, R.F., 1994. Soil color variations along an iron oxide gradient in a mine drainage treatment wetland. Wetlands 14, 243-246.

Tessier, A., Campbell, P.G.C. and Bisson, M., 1979. Sequential extraction procedure for the speciation of particulate trace metals. Anal. Chem. 51(7), 844-851.

Tessier, A., Campbell, P.G.C. and Bisson, M., 1979. Sequential extraction procedure for the speciation of particulate trace metals. Anal. Chem. 51(7), 844-851.

Tipping, E., Hetherington, N.B., Hilton, J., Thompson, D., Bowles, E. and Hamilton-Taylor, J., 1985. Artifacts in the use of selective chemical extraction to determine distributions of metals between oxides of manganese and iron. Anal. Chem. 57, 1944-1946.

Tokalioglu, S., Kartal, S. and Elçi, L., 2000. Determination of heavy metals and their speciation in lake sediments by flame atomic adsorption spectrometry after a four-stage extraction procedure. Anal. Chim. Acta 413, 33-40.

Trivedi, P. and Axe, L., 2000. Modeling Cd and Zn sorption to hydrous metal oxides. Environ. Sci. Technol. 34, 2215-2223.

Trivedi, P., Axe, L. and Tyson, T.A., 2001. XAS studies of Ni and Zn Sorbed to hydrous manganese oxide. Environ. Sci. Technol. 35, 4515-4521.

Turner, D. and McCoy, D., 1990. Anoxic alkaline drain treatment system, a low cost acid mine drainage treatment alternative, In: Proceedings of the National Meeting of the American Society for Surface Mining and Reclamation, Lexington, KY, pp. 73-75.

Ure, A.M., Quevauviller, P.H., Muntau, H. and Griepink, B., 1993. Speciation of heavy metals in soils and sediments. An account of the improvement and harmonization of extraction techniques undertaken under the auspices of the BCR of the Commission of the European Communities. Intern. J. Environ. Anal. Chem. 51, 135-151.

Walton, A.G., 1979. *The Formation and Properties of Precipitates*. Robert E. Krieger Publishing Company, New York, 232 p.

Watzlaf, G.R., Schroeder, K.T. and Kairies, C., 2000. Long-term performance of alkalinity-producing passive systems for the treatment of mine drainage, In: Proceedings of the National Meeting of the American Society for Surface Mining and Reclamation, Tampa, FL, pp. 262-274.

Webster, J.G., Swedlund, P.J. and Webster, K.S., 1998. Trace metal adsorption on acid mine drainage iron (III) oxyhydroxy sulfate. Environ. Sci. Technol. 32(10), 1361-1368.

Wenzel, W.W., Kirchbaumer, N., Prohaska, T., Stingeder, G., Lombi, E. and Adriano, D.C., 2001. Arsenic fractionation in soils using an improved sequential extraction procedure. Anal. Chim. Acta 436, 309-323.

Whalley, C. and Grant, A., 1994. Anal. Chim. Acta 291, 287.

Winters, W.R., Capo, R.C., Wolinsky, M.W., Weaver, T.J. and Hedin, R.S., 1999. Geochemical and hydrogeologic evolution of alkaline discharges from abandoned mines, Sixteenth Annual International Coal conference.

Xu, C.Y., Schwartz, F.W. and Traina, S.J., 1997. Treatment of acid-mine water with calcite and quartz sand. Environ. Engineer. Sci. 14(3), 141-152.

Yates, D.E. and Healy, T.W., 1975. Mechanism of anion sorption at the ferric and chromic oxide/water interfaces. J. Colloid Interface Sci. 52, 222-228.

Zeltner, W.A. and Anderson, M.A., 1988. Surface charge development at the goethite/aqueous solution interface. Effects of CO_2 adsorption. Langmuir 4, 469-474.